



# 1 Introduction

With two-state option pricing models, there is in general no closed form solution except for some payoffs and models, like the stochastic volatility model of HESTON [1993] for a vanilla option or the pricing of an exchangeable option in a Black and Scholes framework. Numerical algorithms are also a key point for 2D option pricing. Three types of numerical methods are available: numerical integration (deterministic, Monte Carlo and quasi-Monte Carlo), finite difference and related fields like finite elements methods, and markov methods (extension of binomial tree in a higher dimension). In this paper, we review these methods and apply them to some option problems.

## 2 Numerical algorithms of 2D option pricing

In the  $M$ -factor arbitrage model which satisfies the standard regularity conditions, the price of the financial asset<sup>1</sup>  $P(t) = P(t, X(t))$  satisfies the following Partial Differential Equation

$$\begin{cases} \frac{1}{2} \text{trace} \left( \Sigma(t, X)^\top P_{XX}(t, X) \Sigma(t, X) \rho \right) \\ + \left[ \mu(t, X)^\top - \lambda(t, X)^\top \Sigma(t, X)^\top \right] P_X(t, X) \\ + P_t(t, X) - r(t, X) P(t, X) + g(t, X) = 0 \\ P(T) = G(T, X(T)) \end{cases} \quad (1)$$

The  $M$ -dimensional state vector  $X$  is a Markov diffusion process taking values in  $\mathcal{R}_X \subset \mathbb{R}^M$  defined by the following stochastic differential equation system

$$\begin{cases} dX(t) = \mu(t, X(t)) dt + \Sigma(t, X(t)) dW(t) \\ X(t_0) = X_0 \end{cases} \quad (2)$$

where  $W(t)$  is a  $N$ -dimensional Wiener process defined on the fundamental probability space  $(\Omega, \mathcal{F}, \mathbb{P})$  with the covariance matrix

$$\mathbb{E} \left[ W(t) W(t)^\top \right] = \rho t \quad (3)$$

Most of the two-state variable models impose  $N = 2$ . In this case, equation (2) becomes

$$\begin{bmatrix} dX_1(t) \\ dX_2(t) \end{bmatrix} = \begin{bmatrix} \mu_1(t, X_1, X_2) \\ \mu_2(t, X_1, X_2) \end{bmatrix} dt + \begin{bmatrix} \sigma_{1,1}(t, X_1, X_2) & \sigma_{1,2}(t, X_1, X_2) \\ \sigma_{2,1}(t, X_1, X_2) & \sigma_{2,2}(t, X_1, X_2) \end{bmatrix} \begin{bmatrix} dW_1(t) \\ dW_2(t) \end{bmatrix} \quad (4)$$

with

$$\rho = \begin{bmatrix} 1 & \rho \\ & 1 \end{bmatrix} \quad (5)$$

and the fundamental equation takes the following form

$$\begin{aligned} & \left[ \frac{1}{2} \sigma_{1,1}^2 + \rho \sigma_{1,1} \sigma_{1,2} + \frac{1}{2} \sigma_{1,2}^2 \right] P_{X_1, X_1} + \left[ \frac{1}{2} \sigma_{2,1}^2 + \rho \sigma_{2,1} \sigma_{2,2} + \frac{1}{2} \sigma_{2,2}^2 \right] P_{X_2, X_2} \\ & + [\sigma_{1,1} \sigma_{2,1} + \rho \sigma_{1,1} \sigma_{2,2} + \sigma_{1,2} \sigma_{2,2} + \rho \sigma_{1,2} \sigma_{2,1}] P_{X_1, X_2} \\ & + [\mu_1 - \lambda_1 \sigma_{1,1} - \lambda_2 \sigma_{1,2}] P_{X_1} + [\mu_2 - \lambda_1 \sigma_{2,1} - \lambda_2 \sigma_{2,2}] P_{X_2} \\ & + P_t - rP + g = 0 \end{aligned} \quad (6)$$

The solution of the equation (6) with the terminal value  $P(T) = G(T, X(T))$  is then given by the Feynman-Kac representation theorem (FRIEDMAN [1975]) :

$$P(t_0) = \mathbb{E}_{\mathbb{Q}} \left[ G(T, X(T)) \exp \left( - \int_{t_0}^T r(t, X(t)) dt \right) + \int_{t_0}^T g(t, X(t)) \exp \left( - \int_{t_0}^t r(s, X(s)) ds \right) dt \middle| \mathcal{F}_{t_0} \right] \quad (7)$$

<sup>1</sup>The maturity date of the asset is  $T$ . The delivery value  $G$  depends on the values taken by the state variables at the maturity date  $G = P(T) = G(T, X(T))$  and the asset pays a continuous dividend  $g$  which is a function of the state vector  $g = g(t, X(t))$ .

with  $\mathbb{Q}$  the *martingale* probability measure. The pricing of *European* options could be done by solving the PDE (6) or by integrating the formula (7). The case of path-dependent option is more complicated, but the price could be found in general with the same techniques.

## 2.1 Numerical integration methods

We consider the example of a Basket/Spread option on two assets. Let  $S_i(t)$  be the price process of the stock  $i$  at time  $t$ . Under the unique equivalent martingale measure  $\mathbb{Q}$  and according to the Black-Scholes model, we assume that the dynamics of  $S_i(t)$  is a log-normal diffusion

$$dS_i(t) = b_i S_i(t) dt + \sigma_i S_i(t) dW_i(t) \quad (8)$$

where  $b_i$  is the cost-of-carry parameter,  $\sigma_i$  the instantaneous volatility and  $E[W_1(t)W_2(t)] = \rho t$ . Using the Cholesky decomposition of the correlation matrix of  $\{W_1(t), W_2(t)\}$ , we could show that the price associated to the payoff  $(\alpha_1 S_1(T) + \alpha_2 S_2(T) - K)^+$  is given by

$$C(t_0) = e^{-r(T-t_0)} \iint_{\mathbb{R}^2} \frac{1}{2\pi} g(\omega_1, \omega_2) \exp\left(-\frac{1}{2}(\omega_1^2 + \omega_2^2)\right) d\omega_1 d\omega_2 \quad (9)$$

with

$$\begin{aligned} g(\omega_1, \omega_2) &= (g_1(\omega_1, \omega_2) + g_2(\omega_1, \omega_2) - K)^+ \\ g_1(\omega_1, \omega_2) &= \alpha_1 S_1(t_0) \exp\left(\left(b_1 - \frac{1}{2}\sigma_1^2\right)(T-t_0) + \sigma_1\sqrt{T-t_0}\omega_1\right) \\ g_2(\omega_1, \omega_2) &= \alpha_2 S_2(t_0) \exp\left(\left(b_2 - \frac{1}{2}\sigma_2^2\right)(T-t_0) + \rho\sigma_2\sqrt{T-t_0}\omega_1 + \sigma_2\sqrt{1-\rho^2}\sqrt{T-t_0}\omega_2\right) \end{aligned} \quad (10)$$

We could reduce the computational complexity because the formula (9) is equivalent to

$$C(t_0) = \int_{\mathbb{R}} \text{BS}\left(S_2^*, K^*, \sigma_2\sqrt{1-\rho^2}, T-t_0, b_2 - \frac{1}{2}\rho^2\sigma_2^2, r\right) d\Phi(\omega_1) \quad (11)$$

with  $S_2^* = \alpha_2 S_2(t_0) \exp(\rho\sigma_2\sqrt{T-t_0}\omega_1)$ ,  $K^* = K - g_1(\omega_1, \omega_2)$ .  $\text{BS}(S_0, K, \sigma, \tau, b, r)$  is the Black-Scholes price of an European option of maturity  $\tau$  and a premium  $K$ .  $S_0$ ,  $\sigma$ ,  $b$  and  $r$  are respectively the current price of the underlying asset, the volatility, the cost-of-carry parameter and the interest rate.

This first example requires to solve the integration problem (9) or (11) with numerical methods. One of the most used methods are certainly quadrature rules (GOLUB and WELSCH [1969]). The underlying idea is to approximate the function by an appropriate polynomial. In the case of Gauss quadratures<sup>2</sup>, Golub and Welsch show that if  $f(x) = B(x)p(x)$  with  $p \in \mathcal{P}_{2n-1}$  ( $\mathcal{P}_n$  is a set of order  $n$  polynomials), then there exist nodes  $0 < x_1 < x_2 < \dots < x_n < 1$  such that  $I = \int_0^1 f(x) dx = \sum_{i=1}^n w_i f(x_i)$  where  $w_i$  are positive weights<sup>3</sup>. If  $f(x)$  is not a polynomial, but is smooth relative to  $p \in \mathcal{P}_{2n-1}$ ,  $\mathcal{G}(f) = \sum_{i=1}^n w_i f(x_i)$  is an approximation of the integral. One of the major issue is of course the accuracy of the approximation. To compute the weights and the nodes, we have to specify the basis function  $B(x)$  and the support.  $\{w_i, x_i\}$  are also the solution of an eigenvalue problem of a Jacobi matrix<sup>4</sup> and are associated to a specific class of polynomials  $\mathcal{P}_{2n-1}$  (see the figure 1). For example, Legendre quadratures are used for finite support and  $B(x) = 1$ . An important point of quadrature methods is that the extension to higher dimensions is straightforward (DAVIS and RABINOWITZ [1984]).

We consider the function  $f(x) = 2\pi\varpi \cos(2\pi\varpi x) + 2x$ . In the figure 2, we have plotted the function  $f$ , the true value of the integral  $\int_0^x f(t) dt = x^2 + \sin(2\pi\varpi x)$  and its numerical approximation for  $\varpi = 1$ . We remark that the approximation depends both on the order  $n$  of the quadrature and the value  $x$  of the

<sup>2</sup>There are other quadrature rules, for example the Gauss-Radau, Gauss-Lobatto or Gauss-Kronrod rules (CALVETTI, GOLUB, GRAGG and REICHEL [1998]).

<sup>3</sup>The extension to other supports is not a difficulty.

<sup>4</sup>Some numerical values could be found in ABRAMOWITZ and STEGUN [1970].

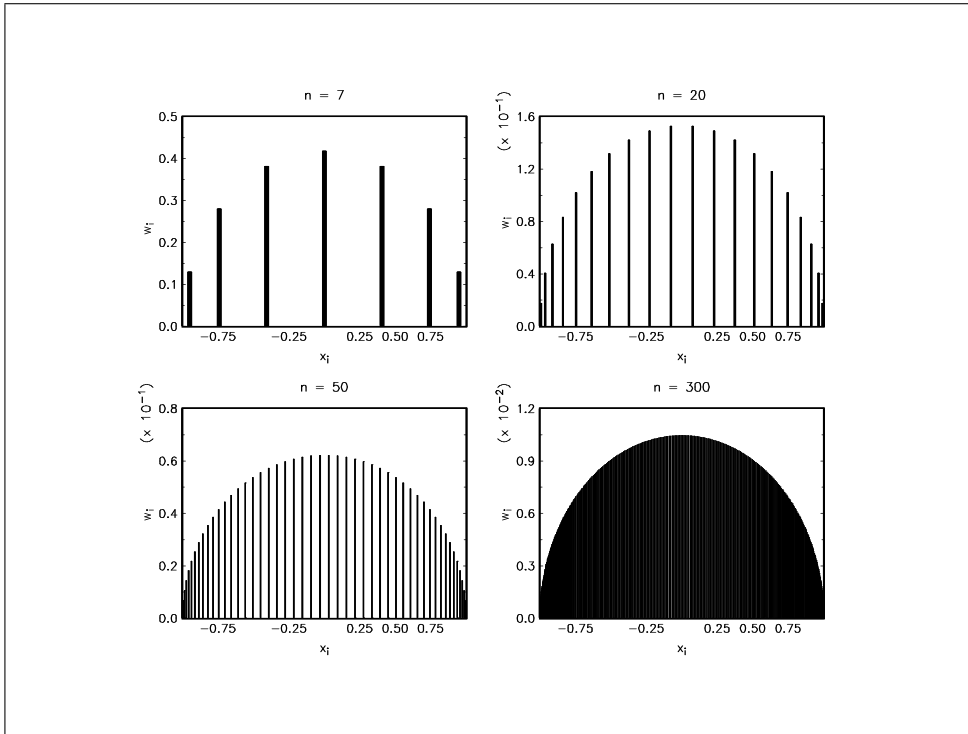


Figure 1: Gauss quadrature nodes and weights

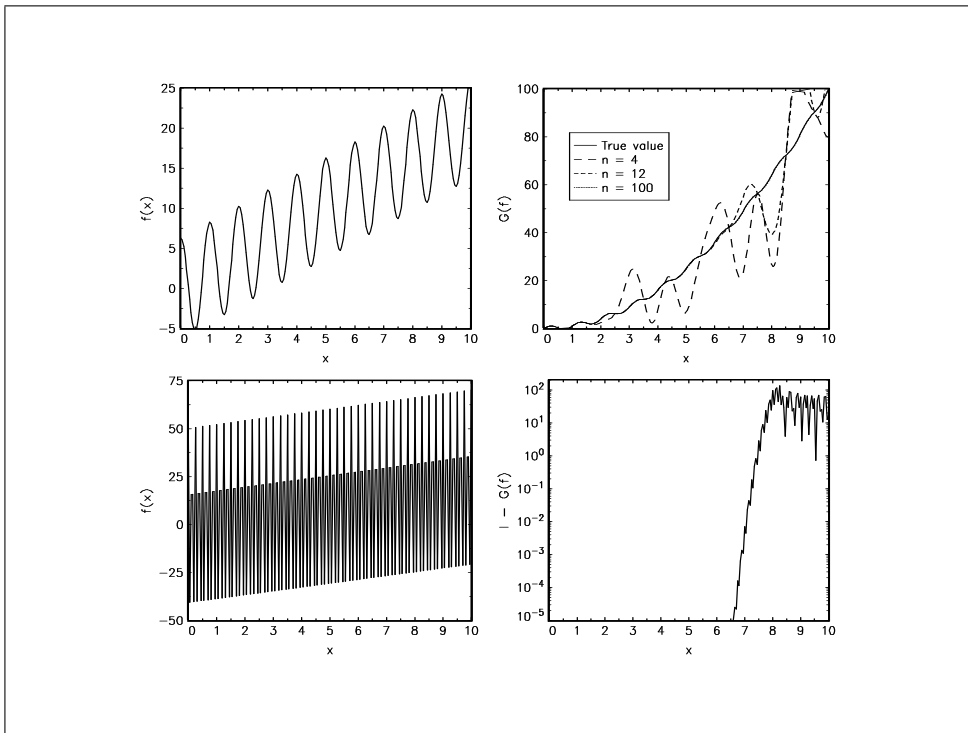


Figure 2: Numerical integration with Gauss-Legendre quadrature

bound. For a fixed  $n$ , the error is in general greater for a bigger value of the bound. In the third and fourth quadrants, we have set  $\varpi$  to 8. To investigate the accuracy of the numerical solution for an order  $n$ , we have to verify that  $f$  is smooth relative to the appropriate polynomial (see the figure 3). For example, if we use an order 200 quadrature rule,  $p \in \mathcal{P}_{399}$ . In our case,  $n = 16$  is not appropriate because  $f$  could not be ‘well-approximated’ for  $x \in [0, 10]$ . We remark also that the error does not decrease systematically with  $n$  (compare  $n = 10$  and  $n = 16$  in the figure 3). Another key point is the problem of not finite support. We have reported in the table (1) the value taken by the last node  $x_n$  for the Gauss-Laguerre and Gauss-Hermite quadratures<sup>5</sup>. The use of such rules implies that the approximations  $\int_0^\infty f(x) dx \simeq \int_0^{x_n} f(x) dx$  and  $\int_{-\infty}^\infty f(x) dx \simeq \int_{-x_n}^{x_n} f(x) dx$  must be valid<sup>6</sup>.

$n$	Laguerre	Hermite
4	9.395	1.650
8	22.86	2.930
16	51.70	4.688
32	111.7	7.125
100	374.9	13.40
200	767.8	19.33

Table 1: Value of the node  $x_n$

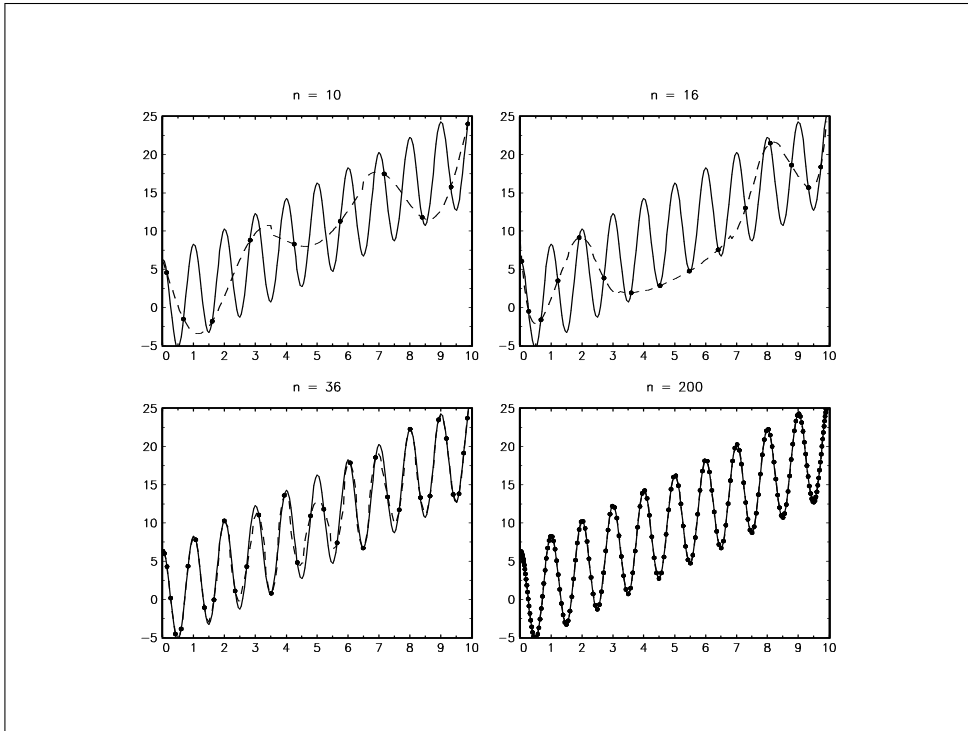


Figure 3: Legendre polynomial interpolation of the function

We consider the pricing of Basket/Spread options. We have reported in the figure (4) the numerical values<sup>7</sup> given by the two-dimensional quadrature methods applied to the equation (9). We remark that a small order  $n$  gives a poor accuracy. If  $n$  is high, there are some computer roundoffs and the price may

<sup>5</sup>The Laguerre and Hermite quadrature methods are used respectively when the support of the integral is  $[0, \infty[$  and  $]-\infty, \infty[$ .

<sup>6</sup>In particular, we remark that if  $f$  is even, it would be not equivalent to compute the integral  $\int_{-\infty}^\infty f(x) dx$  by the two rules with the same order.

<sup>7</sup>The parameters are  $S_1(t_0) = 100$ ,  $b_1 = 6\%$ ,  $\sigma_1 = 20\%$ ,  $S_2(t_0) = 95$ ,  $b_2 = 3\%$ ,  $\sigma_2 = 15\%$ ,  $T - t_0 = 1$  and  $r = 5\%$ .

not converge<sup>8</sup>. One difficulty is that for a fixed  $n$ , we could have a very good approximation for some parameters, whereas the approximation is not good for other parameters. We note moreover that these difficulties becomes harder for higher dimensions.

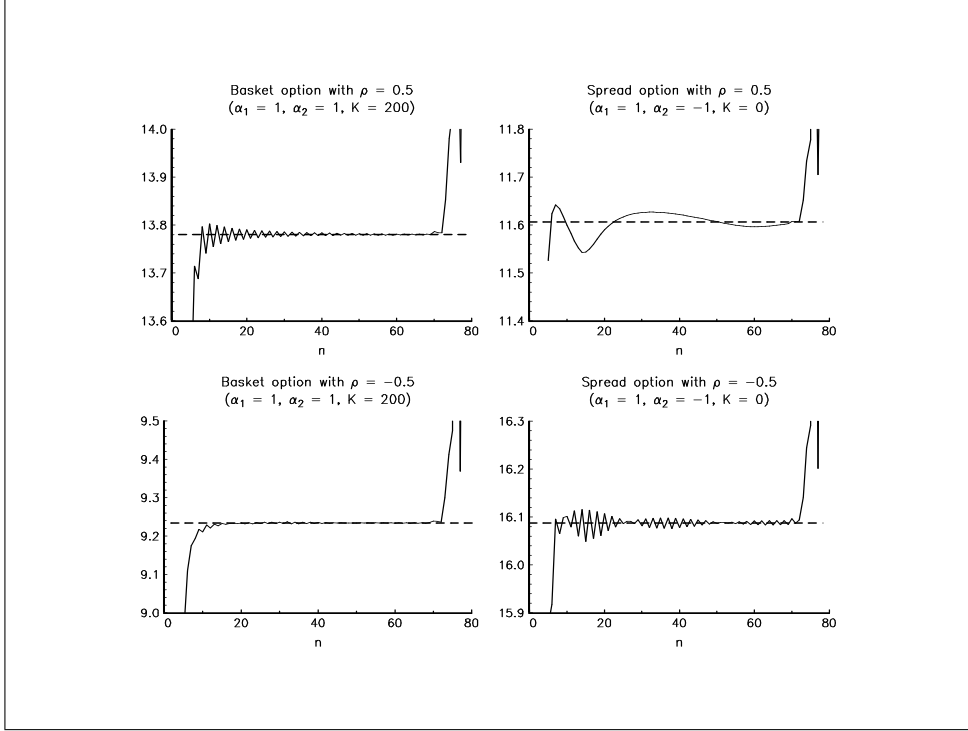


Figure 4: Basket/Spread option prices computation

## 2.2 Monte Carlo and quasi-Monte Carlo methods

Let  $\mathbf{H}$  be a distribution on  $\Omega$  and  $g$  a continuous function. We have also

$$\mathbb{E}[g(\mathbf{X})] = \int_{\Omega} g(\mathbf{x}) d\mathbf{H}(\mathbf{x}) \quad (12)$$

with  $\mathbf{X}$  a random variable with distribution  $\mathbf{H}$ . Then, we have

$$\lim \frac{1}{n} \sum_{i=1}^n g(\mathbf{x}_i) = \int_{\Omega} g(\mathbf{x}) d\mathbf{H}(\mathbf{x}) \quad (13)$$

with  $\mathbf{x}_1, \dots, \mathbf{x}_n$   $n$  iid random variates. Monte Carlo methods are based on the idea that we could transform the problem of integration by a problem of expectation. In the general case, we have  $I = \int_{\Omega} f(\mathbf{x}) d\mathbf{x}$ . We assume that we could decompose  $f(\mathbf{x})$  by  $g(\mathbf{x})h(\mathbf{x})$  with  $h$  a kernel density function. It is also equivalent to compute  $I$  or  $\int_{\Omega} g(\mathbf{x}) d\mathbf{H}(\mathbf{x})$  and we have the following property (GEWEKE [1995]):

$$\text{plim } n^{-1/2} (I_n - I) = \mathcal{N} \left( 0, \int_{\Omega} (g(\mathbf{x}) - I)^2 d\mathbf{H}(\mathbf{x}) \right) \quad (14)$$

with  $I_n = \frac{1}{n} \sum_{i=1}^n g(\mathbf{X}_i)$ . In practice, the sequence  $\{\mathbf{x}_1, \dots, \mathbf{x}_n\}$  is generated by pseudo-random methods such as linear congruential generators (see ENTACHER [1997] for a good review on PRNGs). In this case, the

<sup>8</sup>This comes from the fact that  $w_i w_j$  is very small for large  $n$ .

good properties of Monte Carlo algorithm (“the convergence rate  $n^{-1/2}$  is independent of the dimension of  $\Omega$  and the convergence rate holds even for functions from  $\mathcal{L}_2$ ”) are not always preserved (TRAUB and WOŹNIAKOWSKI [1989]). In practice, the efficiency of Monte Carlo could be improved by using some accelerated methods (by using control or antithetic variates). We take the previous Basket example with  $\rho = 0.5$ . In the figure 5, we have represented the probability density function of  $I_n$  for  $n = 100$  and  $n = 200$ . Moreover, we have reported the corresponding density when we use an antithetic variate (a.v.) with  $n = 100$ .

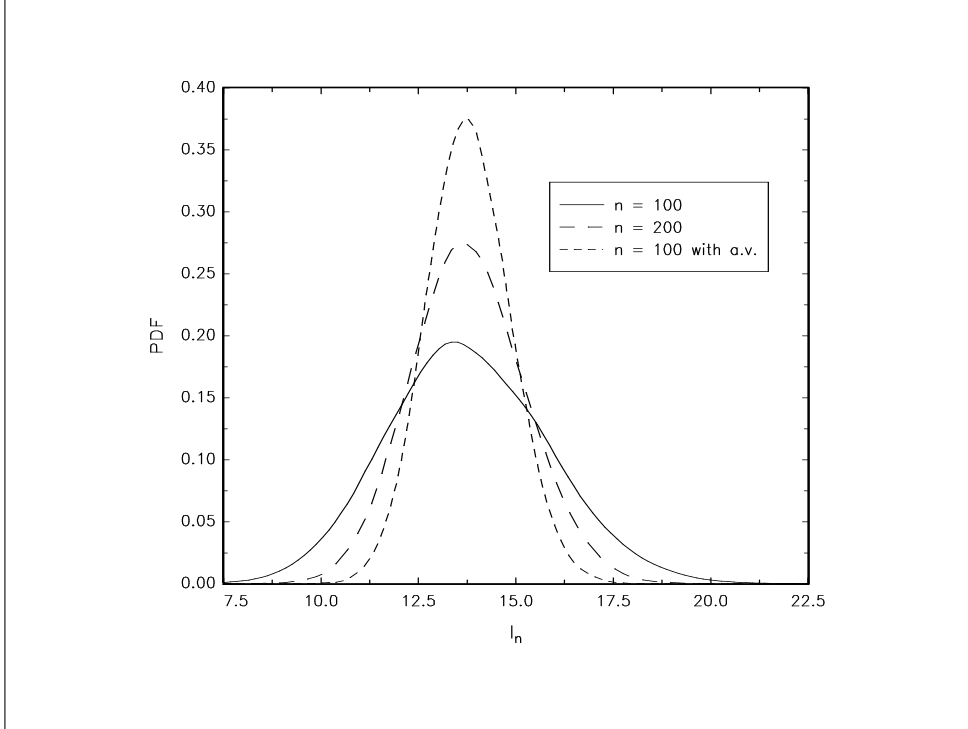


Figure 5: Density of the integral  $I_n$

In 1992, Joseph Traub and his Ph.D. student Spassimir Paskov try to apply quasi-Monte Carlo methods to value a collateralized mortgage obligation, which was a 360 dimensional problem. The project was the following (see [60]):

*Theory suggests that low discrepancy algorithms are sometimes superior to Monte Carlo algorithms. However, a number of researchers report that their numerical tests show that this theoretical advantage decreases with increasing dimension. Furthermore, they report that the theoretical advantage of low discrepancy algorithms disappears for rather modest values of the dimension, say,  $d \leq 30$ . We decided to compare the efficacy of low discrepancy and Monte Carlo algorithms on the evaluation of financial derivatives.*

The idea that “QMC is superior to MC for finance computations” could be found in numerous publications of Traub (see for example [58], [59] or [61]). Before doing some illustrations, we give a brief description of the QMC underlying theory. Without loss of generality, we assume that  $\Omega = [0, 1]^d$  and  $h(\mathbf{x}) = 1$ . With MC methods, we generate uniform random points in the hypercube  $[0, 1]^d$ . QMC methods use non-random points in order to have a more nicely uniform distribution. A low discrepancy sequence  $\mathcal{U} = \{\mathbf{u}_1, \dots, \mathbf{u}_n\}$  is then a set of deterministic points distributed in the hypercube  $[0, 1]^d$ . Let us define the star discrepancy of  $\mathcal{U}$  by  $D_n^*$ :

$$D_n^*(\mathcal{U}) = \sup_{\mathbf{x} \in \Omega} \left| \frac{1}{n} \sum_{j=1}^n \prod_{i=1}^d \chi(1 \leq \mathbf{u}_j^i \leq \mathbf{x}^i) - \prod_{i=1}^d \mathbf{x}^i \right| \quad (15)$$

We could interpret  $D^*$  as a distance measure between the theoretical continuous uniform distribution and the discrete uniform distribution generated by the low discrepancy sequence  $\mathcal{U}$ . We note that if  $\mathcal{U}$  is really uniform, then  $\lim D_n^*(\mathcal{U}) = 0$  for every dimension  $d$ . Moreover, the Koksma-Hlawka inequality implies that

$$|I_n - I| \leq D_n^*(\mathcal{U}) \mathcal{V}(f) \quad (16)$$

where  $\mathcal{V}(f)$  is the Hardy-Krause variation of  $f$  (this result is one of various Chelson's theorems — see SPANIER and LI [1998]). We could find low discrepancy sequences such that the error is of order  $n^{-1} (\ln n)^d$  in probability (this is the best possible bound — see MOROKOFF and CAFLISCH [1994]). If we compare this bound with the order convergence of MC  $O(n^{-1/2})$ , we remark that QMC is theoretically better than MC for small dimensions<sup>9</sup>. For high dimensions, QMC requires a large number of points to be efficient (MOROKOFF and CAFLISCH [1995]). People have done some works to explain the fact that QMC **could be more accurate** than MC even for large dimension  $d$ . Nevertheless, they present only partial answers (SLOAN and WOŹNIAKOWSKI [1998], CAFLISCH, MOROKOFF and OWEN [1997]). Moreover, most of the financial problems, which have been studied, are path-independent contingent claims pricing<sup>10</sup>.

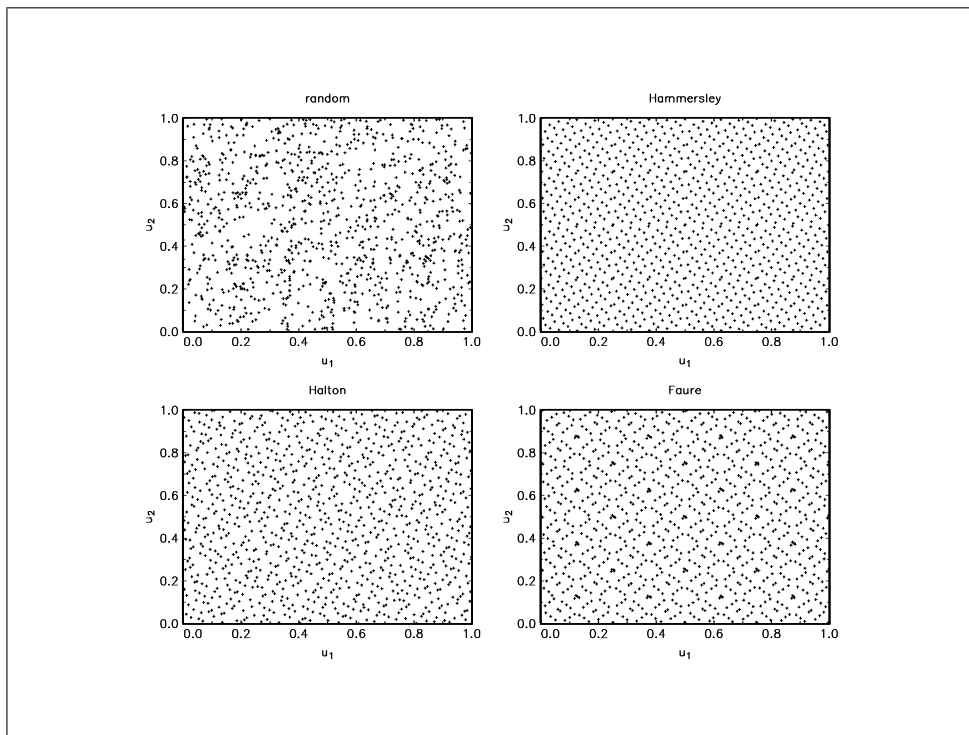


Figure 6: Comparison of different pseudo-random generators

BOULEAU and LÉPINGLE [1994] review different quasi-random sequences<sup>11</sup>. The most known are the Halton', Sobol' and Faure sequences and corresponding computational codes are available in different pro-

<sup>9</sup>However, as noted by LÉMIÉUX and L'ECUYER [2000], “the most useful property of (15) is not to give an idea of the integration error, because the bound is usually too loose, but to derive criteria for choosing good sets  $\mathcal{U}$  by providing a quantity to minimize, namely  $D_n^*(\mathcal{U})$ ”.

<sup>10</sup>For example, ÖKTEN [2000] reports some results on Asian options and European options with stochastic volatility, and the conclusions are not very clear!

<sup>11</sup>There are different methods to construct quasi-random sequences. The most used are lattice rules, digital sequences or  $(t, m, s)$ -nets. OWEN [1998a] defines these last sequences as following:

Let  $t$  and  $m$  be nonnegative integers. A finite sequence  $\mathcal{U} \in [0, 1]^s$  with  $n = b^m$  is a  $(t, m, s)$ -nets in base  $b$  if every  $b$ -ary box of volume  $b^{t-m}$  contains exactly  $b^t$  points of the sequence.

We note also that we could construct ‘new’ quasi-random sequences by using randomization techniques (see OWEN [1998b] for an application of LSS — Latin Supercube sampling).

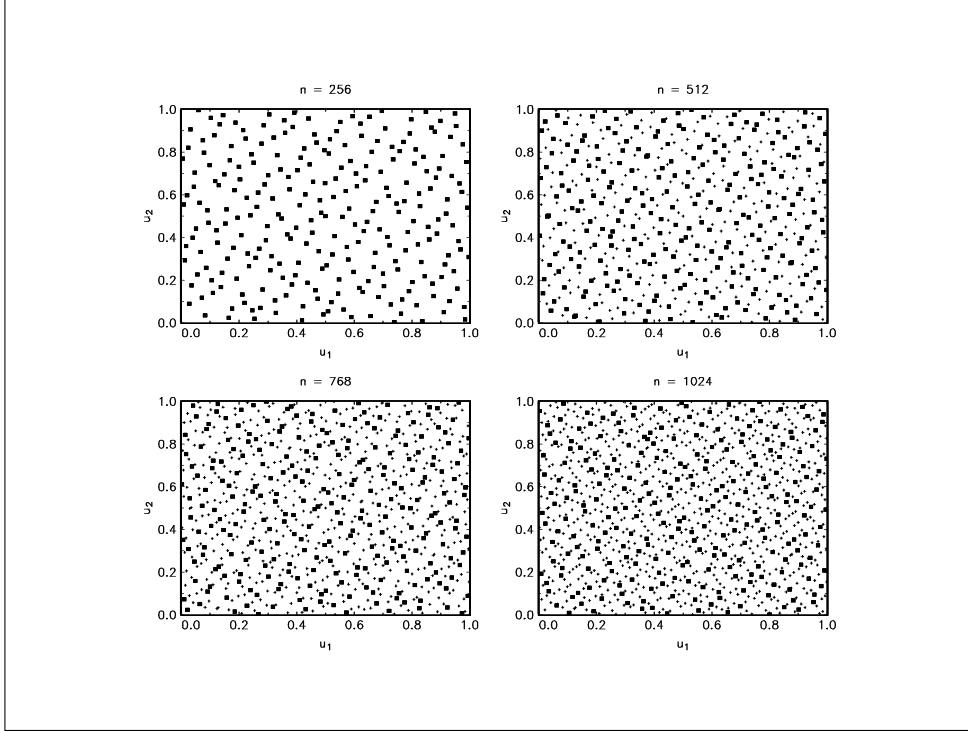


Figure 7: How the Sobol generator works ?

gramming languages (see [12], [13], [62] or [72]). The techniques to generate the sequences are based on number theory. For example, the Halton's sequence is based on the  $p$ -adic expansion of integers  $n = d_k p^k + \dots + d_1 p + d_0$  where  $d_i \in \{0, \dots, p-1\}$  for  $i = 0, \dots, k$  and on the radical-inverse function  $\varrho_b(n) = \sum_{i=0}^k d_i p^{-(i+1)}$  (WANG and HICKERNELL [2000]). The  $d$ -dimensional Halton  $\varrho = \{\varrho_n\}$  sequence is defined by  $\varrho_n = (\varrho_{p_1}(n), \dots, \varrho_{p_d}(n))$  where  $p_1, \dots, p_d$  are integers that are greater than 1 and pairwise relatively prime<sup>12</sup>. We have represented this sequence and two others<sup>13</sup> (Hammersley and Faure) in the figure 6. The idea is of course to add the new points not randomly, but 'between the existing points'. For example, we have added 256 points in the Sobol sequence in each quadrant of the figure 7 — the new points correspond to a square symbol. Now, suppose that the dimension  $d$  becomes larger. It will become more and more difficult to fill the hypercube<sup>14</sup>. To illustrate this problem, we consider the 3D projection of a  $d$ -dimensional normal variates obtained using the first 3072 points of the Faure sequences<sup>15</sup>. We remark that we have to increase the number of points if we would like to map all the space. And we have to be careful if we do not want to generate some 'hole area' (see the figure 9 which represents the first 1024 points of the directional vectors on the unit sphere).

We now consider an illustration. The problem is the pricing of a vanilla option in the Black-Scholes model. It assume that the price  $S(t)$  is a log-normal diffusion given by the equation (8). The value of the Call option is then  $C(t_0) = e^{-r(T-t_0)} \mathbb{E}_{\mathbb{Q}} \left[ (S(T) - K)^+ \mid \mathcal{F}_{t_0} \right]$ . The process  $S(T) \mid \mathcal{F}_{t_0}$  is simulated by an

<sup>12</sup>In practice, they are the first  $n$  prime numbers.

<sup>13</sup>We have used  $p_1 = 2$  and  $p_2 = 3$ .

<sup>14</sup>This phenomenon is called 'the curse of dimensionality'.

<sup>15</sup>The mean vector is null and the covariance matrix  $\Sigma$  is

$$\Sigma = \begin{bmatrix} 1 & 0.5 & 0.25 \\ 0.5 & 1 & 0.25 \\ 0.25 & 0.25 & 1 \end{bmatrix}$$

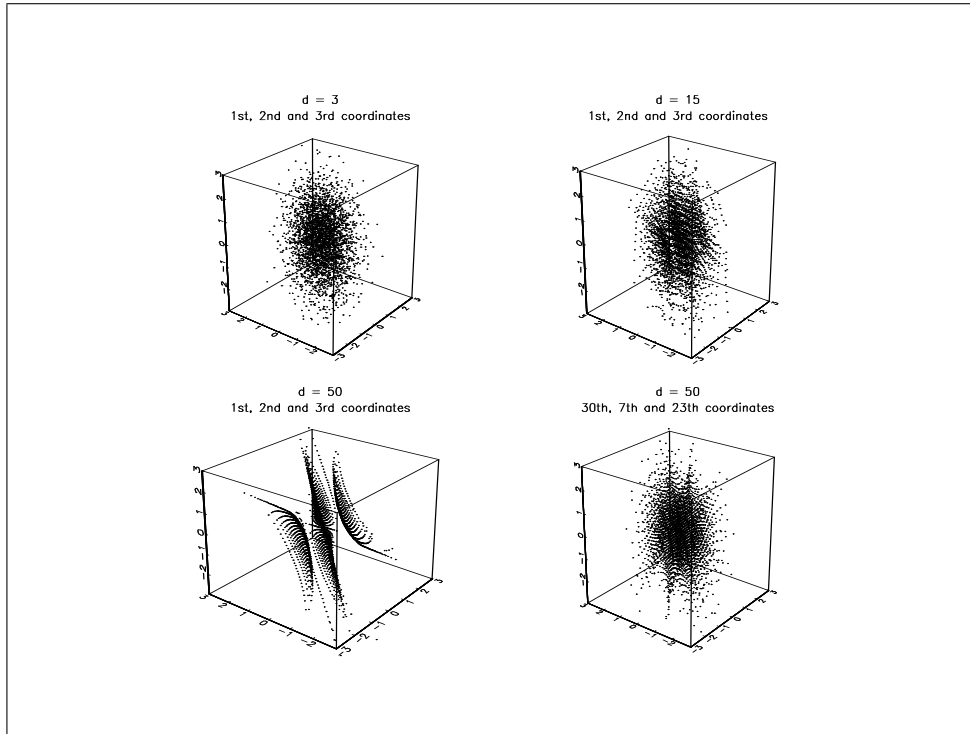


Figure 8: 3D projection of normal pseudo-random numbers with Faure generator

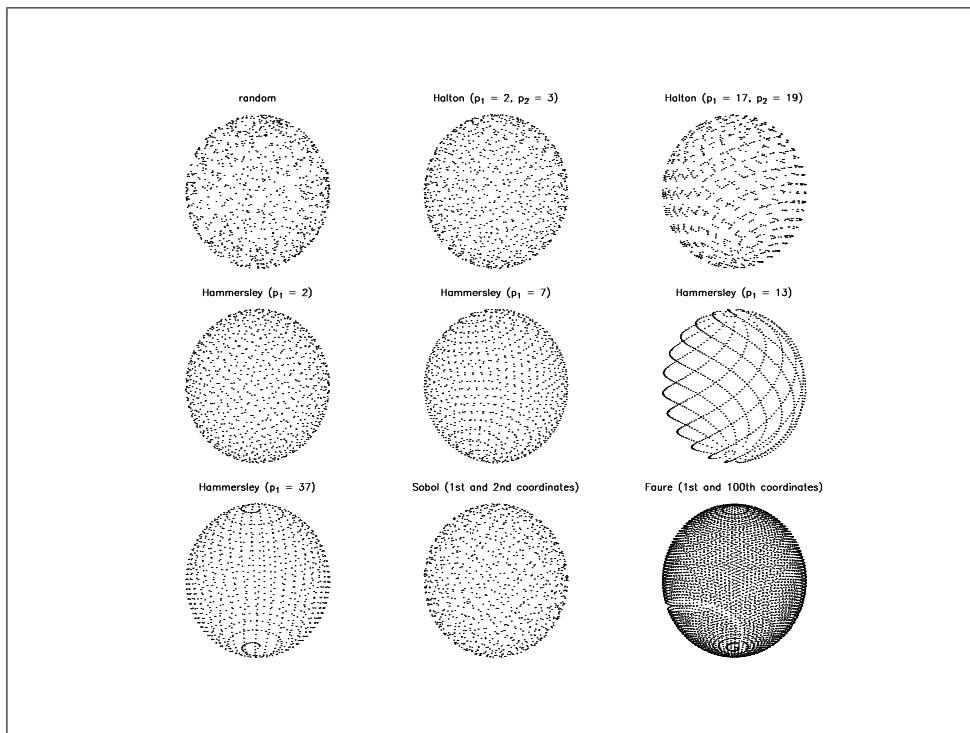


Figure 9: Quasi-random points on the unit sphere

exact scheme (KLOEDEN and PLATEN [1992]) using this recursive formula

$$\ln S(t_{m+1}) = \ln S(t_m) + \left(b - \frac{1}{2}\sigma^2\right)(t_{m+1} - t_m) + \sigma\sqrt{t_{m+1} - t_m}\varepsilon \quad (17)$$

with  $\varepsilon$  a  $\mathcal{N}(0, 1)$  variate and the time discretisation<sup>16</sup>  $t_0 < t_1 < \dots < t_m < \dots < t_{N_t} = T$ . We consider a 5 points discretisation<sup>17</sup>. We have plotted the convergence<sup>18</sup> in the figure 10. Because the Hammersley nets are a closed sequence, we have reported only the last value. We remark the very good behaviour of the Sobol sequence. For the random sequences, the convergence depends on the seed value and on the LCG parameters. Now, we suppose that **the BS option pricing is just one component of a bigger MC problem**<sup>19</sup>. In the figure 10, we show the influence of the dimension  $d$  of the Faure sequence on the convergence. This example is interesting because it illustrates the problem of the curse of dimensionality (see the convergence for the dimension 5000).

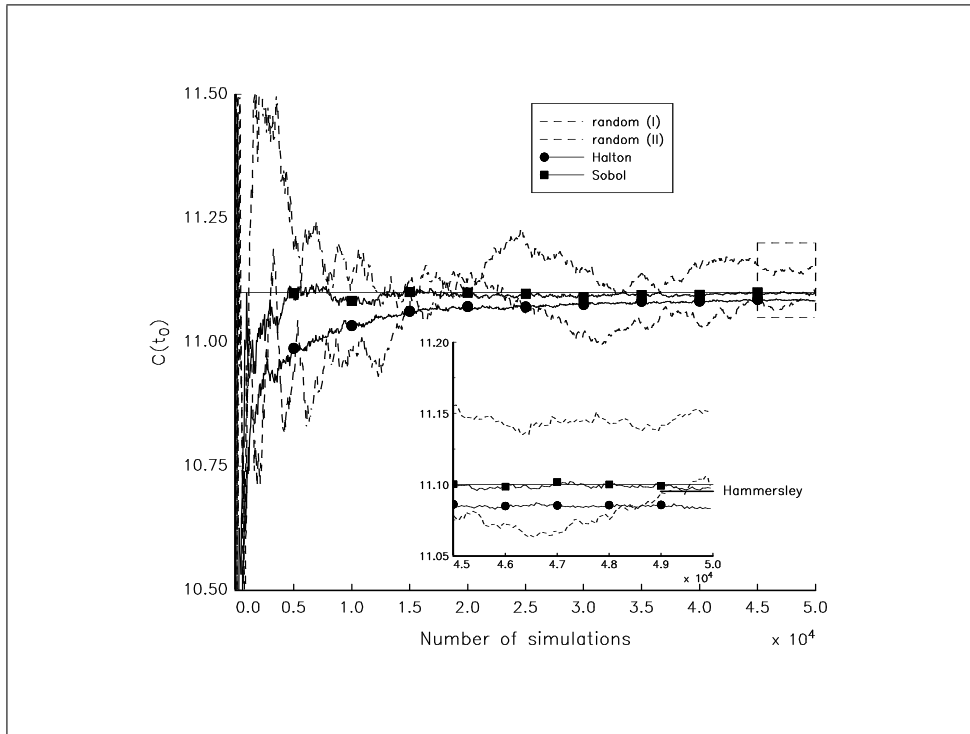


Figure 10: Convergence of QMC methods

Another difficulty is the choice of the quasi-random sequence. For example, we have computed the previous Basket/Spread prices with 32768 simulations and we obtain the results of the table 2. For this example, the prices are the same with a 2 digits precision, because we have a low dimension problem. However, it is not always the case with bigger dimension. The choice of the quasi-random sequence is then important. **But the best method does not exist. A sequence may have a very good behaviour for one problem, and may be less performant for another problem** (see BIRGE [1994] or ÖKTEN [2000] for some illustrations).

In concluding remarks, we could say that, even if there are a lot of works on this research area, we need more research to obtain more convincing results on Quasi-Monte Carlo methods.

<sup>16</sup> $N_t$  is the number of discretisation points for  $t$ .

<sup>17</sup>The dimension  $d$  is also equal to 5.

<sup>18</sup>The parameters are the following:  $S(t_0) = 100$ ,  $K = 100$ ,  $b = 6\%$ ,  $\sigma = 20\%$ ,  $T - t_0 = 1$  and  $r = 5\%$ .

<sup>19</sup>The simulated prices are computed with the first five coordinates of the sequence, whereas the dimension  $d$  of the problem is large.

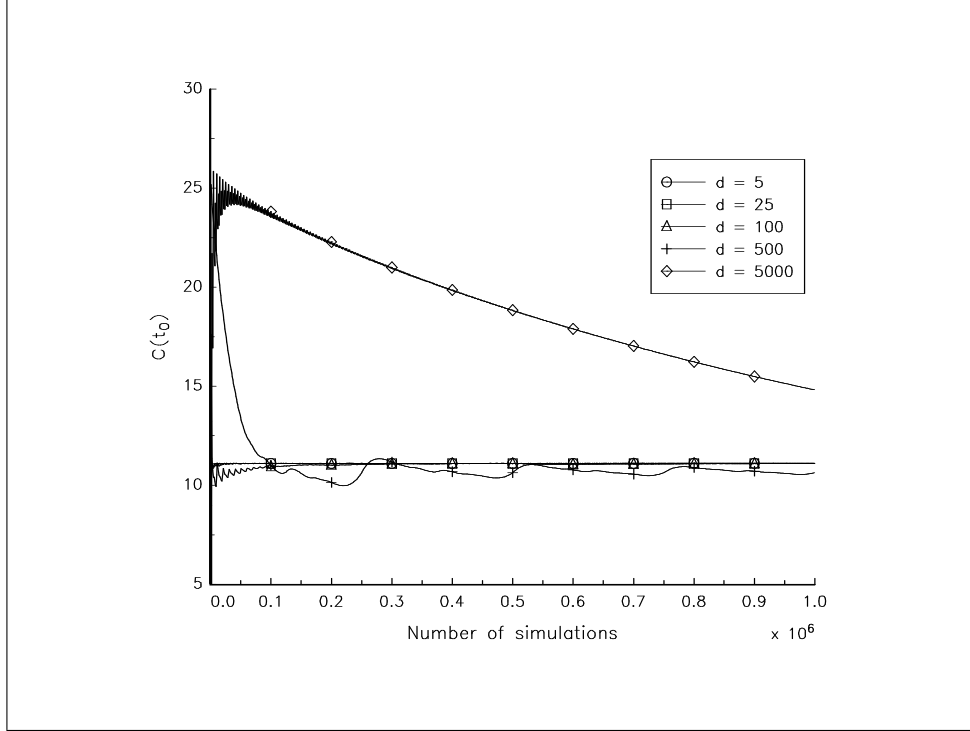


Figure 11: Influence of the dimension  $d$  on the convergence of the Faure QMC prices

	Hermite 32	Hammersley	Halton	Sobol	Faure
$(\alpha_1 = 1, \alpha_2 = 1, \rho = 0.5, K = 200)$	13.785	13.781	13.773	13.776	13.777
$(\alpha_1 = 1, \alpha_2 = -1, \rho = 0.5, K = 0)$	11.627	11.602	11.610	11.608	11.606
$(\alpha_1 = 1, \alpha_2 = 1, \rho = -0.5, K = 200)$	9.2368	9.2291	9.2248	9.2278	9.2277
$(\alpha_1 = 1, \alpha_2 = -1, \rho = -0.5, K = 0)$	11.627	11.602	11.610	11.608	11.606

Table 2: Basket/Spread QMC prices

### 2.3 Finite Difference methods

In this paragraph, we follow the paper of KURPIEL and RONCALLI [1999]. We consider the linear parabolic equation

$$\frac{\partial u(t, x, y)}{\partial t} + f(t, x, y)u(t, x, y) = \mathcal{A}_t u(t, x, y) + g(t, x, y) \quad (18)$$

where  $\mathcal{A}_t$  is the general two dimensional differential operator

$$\begin{aligned} \mathcal{A}_t u(t, x, y) = & a(t, x, y) \frac{\partial^2 u(t, x, y)}{\partial x^2} + 2b(t, x, y) \frac{\partial^2 u(t, x, y)}{\partial x \partial y} + c(t, x, y) \frac{\partial^2 u(t, x, y)}{\partial y^2} + \\ & d(t, x, y) \frac{\partial u(t, x, y)}{\partial x} + e(t, x, y) \frac{\partial u(t, x, y)}{\partial y} \end{aligned} \quad (19)$$

The idea is to solve (18) in a region of the  $(t, x, y)$  space given by  $\mathfrak{T} \times \mathfrak{R}$  where  $\mathfrak{R}$  is a closed region of the  $(x, y)$  plane with a continuous boundary  $\partial \mathfrak{R}$ . In particular, for convenient computation, we assume that  $\mathfrak{R} = [x^-, x^+] \times [y^-, y^+]$  and  $\mathfrak{T} = [t^-, t^+]$ . To solve (18) numerically, we need to impose some boundary conditions. For  $t = t^-$ , we consider a Cauchy condition. For the other boundary, we could choose between a Dirichlet or a Neumann condition. In order to develop a numerical solution for (18), we need to discretise the process  $u(t, x, y)$  in both time and space dimensions. Let  $N_t$ ,  $N_x$  and  $N_y$  be the number of discretisation points for  $t$ ,  $x$  and  $y$  respectively. We denote by  $k$ ,  $h_x$  and  $h_y$  the mesh spacings in time and space in the

$x$  and  $y$  directions respectively<sup>20</sup>. We note  $t_m = t^- + m \cdot k$ ,  $x_i = x^- + i \cdot h_x$  and  $y_j = y^- + j \cdot h_y$ . Let  $u_{i,j}^m$  be the approximate solution to (18) at the grid point  $(t_m, x_i, y_j)$  and  $u(t_m, x_i, y_j)$  the exact solution of the Partial Differential Equation at this point. Let  $M$  be the matrix with  $(i, j)$  entry  $(M_{i,j})$  and denote  $\text{vec}(M)$  by  $\mathbf{m}$ .

The explicit form of equation (18) is

$$\frac{u_{i,j}^{m+1} - u_{i,j}^m}{k} + f_{i,j}^m u_{i,j}^m = \mathbf{A}_{i,j}^m + g_{i,j}^m \quad (20)$$

while the implicit form is

$$\frac{u_{i,j}^{m+1} - u_{i,j}^m}{k} + f_{i,j}^{m+1} u_{i,j}^{m+1} = \mathbf{A}_{i,j}^{m+1} + g_{i,j}^{m+1} \quad (21)$$

Introducing theta-schemes gives

$$\begin{aligned} (1 + k\theta_{i,j}^{m+1} f_{i,j}^{m+1}) u_{i,j}^{m+1} &- k\theta_{i,j}^{m+1} (\mathbf{A}_{i,j}^{m+1} + g_{i,j}^{m+1} + p_{i,j}^{m+1}) \\ &= (1 - k\theta_{i,j}^m f_{i,j}^m) u_{i,j}^m + k\theta_{i,j}^m (\mathbf{A}_{i,j}^m + g_{i,j}^m + p_{i,j}^m) \end{aligned} \quad (22)$$

with

$$\theta_{i,j}^{m+1} + \theta_{i,j}^m = 1 \quad (23)$$

We can show that there exists a square matrix  $H_m$  and a vector  $\mathbf{p}_m$  such that

$$\mathbf{A}^m = H_m \mathbf{u}_m + \mathbf{p}_m \quad (24)$$

We call  $p_{i,j}^m$  the residual absorption function. Then, we have

$$\begin{aligned} [I + k\Theta_{m+1} \mathbf{f}_{m+1} - k\Theta_{m+1} H_{m+1}] \mathbf{u}_{m+1} &= [I - k\Theta_m \mathbf{f}_m + k\Theta_m H_m] \mathbf{u}_m + \\ &k[\Theta_{m+1} \mathbf{g}_{m+1} + \Theta_m \mathbf{g}_m] + k[\Theta_{m+1} \mathbf{p}_{m+1} + \Theta_m \mathbf{p}_m] \end{aligned} \quad (25)$$

with

$$\Theta_m = \text{diag}(\theta_m)$$

and

$$\theta_m = (\theta_{i,j}^m)$$

The equation (25) is the general vec form of finite difference methods for two-dimensional Partial Differential Equations. We have now to specify  $\mathbf{A}_{i,j}^m$  and  $\Theta_m$ . The general form of  $\mathbf{A}_{i,j}^m$  is

$$\mathbf{A}_{i,j}^m = \sum_{\tilde{i}=-2}^2 \sum_{\tilde{j}=-2}^2 \delta_{i,j,\tilde{i},\tilde{j}}^m u_{i+\tilde{i},j+\tilde{j}}^m \quad (26)$$

Then, we can write the matrix  $\mathbf{A}^m$  with elements  $(\mathbf{A}_{i,j}^m)$  in the following form

$$\mathbf{A}^m = \Delta_m \mathbf{u}_m + \mathbf{q}_m \quad (27)$$

In fact,  $\mathbf{q}_m$  reflects the boundary conditions. When we use them, we can split the vector  $\mathbf{q}_m$  and have

$$\mathbf{q}_m = \Lambda_m \mathbf{u}_m + \mathbf{p}_m \quad (28)$$

Then, it is clear that  $H_m$  in equation (25) is

$$H_m = \Delta_m + \Lambda_m \quad (29)$$

The nature of the boundary conditions is important, because a Dirichlet condition will influence the  $\mathbf{p}_m$  vector while a Neuman condition will affect the  $\Lambda_m$  matrix. This integration of the boundary conditions is completely explained in KURPIEL and RONCALLI [1999].

<sup>20</sup>Then, we have  $k = \frac{t^+ - t^-}{N_t - 1}$ ,  $h_x = \frac{x^+ - x^-}{N_x - 1}$  and  $h_y = \frac{y^+ - y^-}{N_y - 1}$ .

Let  $\tau = T - t$  be the time to maturity of the asset. We see that equation (6) could be put in the form (18). In this case,  $\tau$  takes the role of the variable  $t$  and  $X_1$  and  $X_2$  correspond to the  $x$  and  $y$  variables. We have

$$\begin{aligned}
a(\tau, X_1, X_2) &= \frac{1}{2}\sigma_{1,1}^2 + \rho_{1,2}\sigma_{1,1}\sigma_{1,2} + \frac{1}{2}\sigma_{1,2}^2 \\
b(\tau, X_1, X_2) &= \frac{1}{2}(\sigma_{1,1}\sigma_{2,1} + \rho_{1,2}\sigma_{1,1}\sigma_{2,2} + \sigma_{1,2}\sigma_{2,2} + \rho_{1,2}\sigma_{1,2}\sigma_{2,1}) \\
c(\tau, X_1, X_2) &= \frac{1}{2}\sigma_{2,1}^2 + \rho_{1,2}\sigma_{2,1}\sigma_{2,2} + \frac{1}{2}\sigma_{2,2}^2 \\
d(\tau, X_1, X_2) &= \mu_1 - \lambda_1\sigma_{1,1} - \lambda_2\sigma_{1,2} \\
e(\tau, X_1, X_2) &= \mu_2 - \lambda_1\sigma_{2,1} - \lambda_2\sigma_{2,2} \\
f(\tau, X_1, X_2) &= r(T - \tau, X_1, X_2) \\
g(\tau, X_1, X_2) &= g(T - \tau, X_1, X_2) \\
u(0, X_1, X_2) &= G(T, X_1, X_2)
\end{aligned}$$

### 2.3.1 Hopscotch methods

GOURLAY [1970] introduced a class of, so called, *Hopscotch* algorithms to solve parabolic and elliptic partial differential equations of the form (18). The reader could review the article of KURPIEL and RONCALLI [1999] for a complete exposition of these methods. An hopscotch algorithm is defined by a  $\theta$  hopscotch method for some choice of the  $\Theta_m$  matrix and a *filling* hopscotch method following from the  $\delta_{i,j}^m$  definition. The underlying idea is to introduce more sparsity into the linear system (25) — of the form  $\Psi_{m+1}\mathbf{u}_{m+1} = \phi_{m+1}$  — than the classical  $\theta$ -schemes, and in the same time to verify the stability property<sup>21</sup> (GOURLAY and MCGUIRE [1971]). The most popular algorithms are the “ordered odd-even” and the “line” hopscotch schemes. To illustrate them, we have reported ‘a spy plot’ of the equation (25) in the figure 12.

One of the big difficulty is of course to solve the linear system. KURPIEL and RONCALLI [1999] propose to code the matrices into a band form, and then to solve the system with a sparse solver. In the GAUSS implementation [64], they use the LSQR algorithm of PAIGE and SAUNDERS [1982]. LSQR is a conjugate gradient method with refinements which may solves linear equations, minimum length, least squares and regularized least squares problems. The form of the general problem is

$$\min \|A\mathbf{x} - b\|^2 + \|\delta\mathbf{x}\|^2 \quad (30)$$

with  $A$  a general matrix. With CG algorithms, the solution is given by an iterative method  $x_{i+1} = x_i + r_i$  (GOLUB and VAN LOAN [1989]). The algorithm developed by Paige and Sauders is based on *Krylov* methods (IPSEN and MEYER [1988]). It is not the fastest CG method, but it is consistent even if the linear system is not well-conditioned. Moreover, under some assumptions on the mesh spacing, we know that  $\mathbf{u}_{m+1} = \mathbf{u}_m + O(k)$ . We could also replace the system (25) by

$$\begin{aligned}
[I + k\Theta_{m+1}\mathbf{f}_{m+1} - k\Theta_{m+1}H_{m+1}]\mathbf{v}_{m+1} &= (k[\Theta_{m+1}H_{m+1} + \Theta_m] - k[\Theta_{m+1}\mathbf{f}_{m+1} + \Theta_m\mathbf{f}_m])\mathbf{u}_m \\
&\quad k[\Theta_{m+1}\mathbf{g}_{m+1} + \Theta_m\mathbf{g}_m] + k[\Theta_{m+1}\mathbf{p}_{m+1} + \Theta_m\mathbf{p}_m] \quad (31)
\end{aligned}$$

with  $\mathbf{u}_{m+1} = \mathbf{v}_{m+1} + \mathbf{u}_m$ . The form of the linear system is then  $\Psi_{m+1}\mathbf{v}_{m+1} = \Upsilon_{m+1}$  with  $\Upsilon_{m+1} = \phi_{m+1} - \Psi_{m+1}\mathbf{u}_m$ . This formulation does not reduce the dimension of the associated Krylov space  $\mathcal{K}_\varphi(\Psi_{m+1}, \Upsilon_{m+1})$ , but the convergence is faster because the null vector is a more appropriate starting value for this second linear system.

### 2.3.2 Other numerical solvers

There are a lot of other numerical solvers (for example MoL, LOD, ADI or FEM). The *Method of Lines* (MoL) converts the PDE problem into a system of first order ordinary differential equations. The *Locally*

<sup>21</sup>However, we have remarked that the “ordered odd-even” and the “line” hopscotch methods give different results on parabolic and elliptic problems. For parabolic problems, “ordered odd-even” and “line” schemes are comparable to a full Crank-Nicholson scheme. For elliptic problems, the “ordered odd-even” method seems to be less accurate.

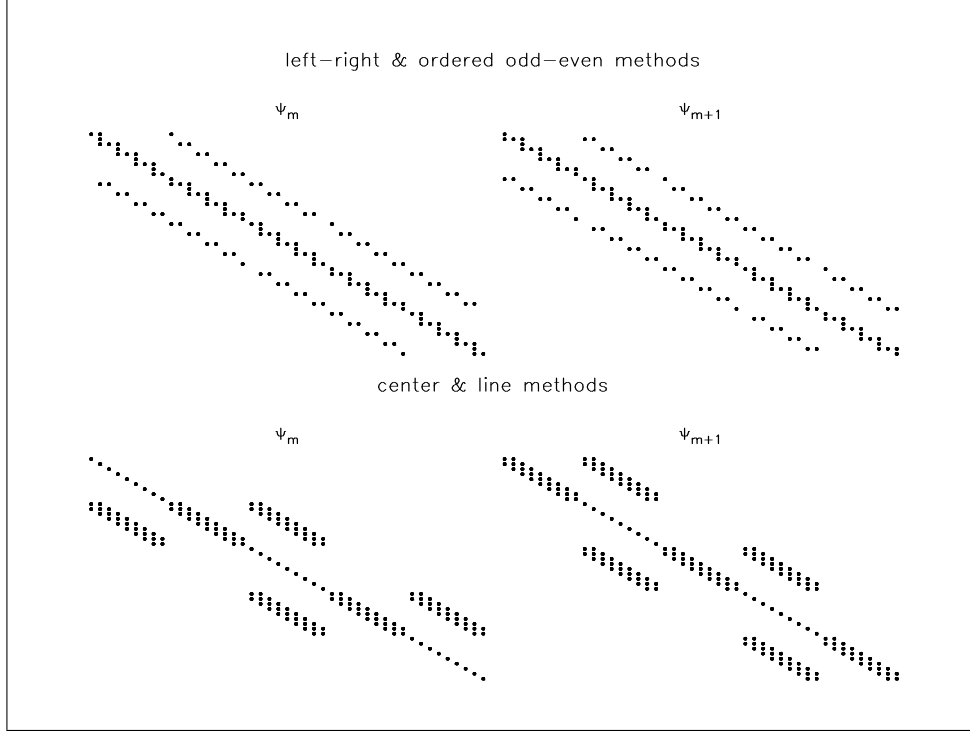


Figure 12: ‘Spy Plot’ of the PDE linear system

*One-Dimensional* (LOD) and *Alternative Direction Implicit* (ADI) algorithms are special cases of Operator Splitting Methods (PRESS, TEUKOLSKY, VETTERLING and FLANNERY [1992]). To understand the basic ideas behind these methods, we consider the classical heat equation

$$\partial_t u(t, x, y) = \partial_{xx} u(t, x, y) + \partial_{yy} u(t, x, y) \quad (32)$$

**Method of Lines** — Using the centered difference approximation<sup>22</sup>, we have

$$\frac{du_{i,j}(t)}{dt} = \delta_{xx} u_{i,j}(t) + \delta_{yy} u_{i,j}(t), \quad \text{for } i = 1, \dots, N_x \text{ and } j = 1, \dots, N_y \quad (33)$$

The vec form of this equation is then

$$\frac{d\mathbf{u}(t)}{dt} = \mathbf{A}\mathbf{u}(t) + \mathbf{b}(t) \quad (34)$$

We obtain also a system of  $N_x \times N_y$  ODE’s, which could be solve by numerical methods (STOER and BURLISH [1993]). One of the success of the MoL algorithm is the possibility of mixing easily different boundary specifications. Moreover, if we use Runge-Kutta methods or explicit Predictor-Corrector methods, we remark that solving the PDE problem requires just matrix-by-vector products, which could be done in a sparse framework. One example of financial application of MoL is MEYER and HOEK [1997].

**Locally One-Dimensional** — A finite difference approximation of (32) is

$$\frac{u_{i,j}^{m+1} - u_{i,j}^m}{k} = \frac{u_{i+1,j}^m - 2u_{i,j}^m + u_{i-1,j}^m}{h_x^2} + \frac{u_{i,j+1}^m - 2u_{i,j}^m + u_{i,j-1}^m}{h_y^2} \quad (35)$$

LEVEQUE [1988] introduces LOD and ADI algorithms in the following way:

<sup>22</sup>We have  $\delta_{xx} u_{i,j}(t) = \frac{u_{i+1,j}(t) - 2u_{i,j}(t) + u_{i-1,j}(t)}{h_x^2}$  and  $\delta_{yy} u_{i,j}(t) = \frac{u_{i,j+1}(t) - 2u_{i,j}(t) + u_{i,j-1}(t)}{h_y^2}$ . Note that the method uses in general more adapted finite difference formulas (see FORNBERG [1998]).

Rather than solving the coupled sparse matrix equation for all the unknowns on the grid simultaneously as in (35), an alternative approach is to replace this fully-coupled single time step by a sequence of steps, each of which is coupled in only one space direction, resulting in a set of tridiagonal systems which can be solved much easily.

For the LOD method, we have

$$\left\{ \begin{array}{l} \frac{u_{i,j}^{m+\frac{1}{2}} - u_{i,j}^m}{\frac{k}{2}} = \frac{u_{i+1,j}^m - 2u_{i,j}^m + u_{i-1,j}^m}{h_x^2} + \frac{u_{i+1,j}^{m+\frac{1}{2}} - 2u_{i,j}^{m+\frac{1}{2}} + u_{i-1,j}^{m+\frac{1}{2}}}{h_x^2} \\ \frac{u_{i,j}^{m+1} - u_{i,j}^{m+\frac{1}{2}}}{\frac{k}{2}} = \frac{u_{i,j+1}^{m+\frac{1}{2}} - 2u_{i,j}^{m+\frac{1}{2}} + u_{i,j-1}^{m+\frac{1}{2}}}{h_y^2} + \frac{u_{i,j+1}^{m+1} - 2u_{i,j}^{m+1} + u_{i,j-1}^{m+1}}{h_y^2} \end{array} \right. \quad (36)$$

**Alternative Direction Implicit** — There are different ADI schemes. One of the most used is the Peaceman-Rachford process:

$$\left\{ \begin{array}{l} \frac{u_{i,j}^{m+\frac{1}{2}} - u_{i,j}^m}{\frac{k}{2}} = \frac{u_{i,j+1}^m - 2u_{i,j}^m + u_{i,j-1}^m}{h_y^2} + \frac{u_{i+1,j}^{m+\frac{1}{2}} - 2u_{i,j}^{m+\frac{1}{2}} + u_{i-1,j}^{m+\frac{1}{2}}}{h_x^2} \\ \frac{u_{i,j}^{m+1} - u_{i,j}^{m+\frac{1}{2}}}{\frac{k}{2}} = \frac{u_{i+1,j}^{m+\frac{1}{2}} - 2u_{i,j}^{m+\frac{1}{2}} + u_{i-1,j}^{m+\frac{1}{2}}}{h_x^2} + \frac{u_{i,j+1}^{m+1} - 2u_{i,j}^{m+1} + u_{i,j-1}^{m+1}}{h_y^2} \end{array} \right. \quad (37)$$

“With this method, each of the two steps involves diffusion in both the  $x$ - and  $y$ -directions. In the first step the diffusion in  $x$  is modelled implicitly while diffusion in  $y$  is modelled explicitly, with the roles reversed in the second step” (LEVEQUE [1988]). A financial application could be found in VILLENEUVE and ZANETTE [1998].

**Finite Element Method** — WILMOTT, DEWYNNE and HOWISON [1993] is a good introduction on this subject. The main idea is to approximate  $u(t, x, y)$  by linear combinations of basis functions (or shape functions)

$$u(t, x, y) = \sum_{l=1}^L c_l \phi_l(t, x, y) \quad (38)$$

Hence, we have to find the nodal values  $\{c_l\}$  solution of a  $L \times L$  linear system. This method is popular in more than one dimensional PDE problem, because FEM could be used with irregular grids and gives smooth solutions (see BUSCA [1999] for an application to optimal exercise policy for American options).

## 2.4 Parallel implementation

To finish this section, we will give some remarks on parallel implementation, which is one of the big issue of 2D (and more) option pricing. There is now a lot of numerical library specially designed for distributed memory parallel computers (GOLUB and ORTEGA [1993]). In particular, the BLAS routines have been rewritten to support distributed memory. PBLAS is now the core of many software, for example ScaLAPACK and IMSL Fortran 90 MP. Parallel implementation of Quadrature and Monte Carlo methods<sup>23</sup> are feasible — see the book of FOX, MESSINA and WILLIAMS [1994] or the HPF implementation of path-integral of option pricing described by MAKIVIC [1995]. It seems that it could be also the case for some QMC methods (for example, Halton’ and Hammersley sequences). Even for parallel solution of PDE, there exist some codes and parallel implementation of sparse methods are now available (see SAAD [1996,1998]).

## 3 Some stopping time problems

In a fully parametrized two-state model, which verifies the standard regularity conditions, the price of an American option satisfies a two-dimensional variational inequality. The variational inequality can then be solved by *hopscotch*, and the optimal boundary can be recovered from the solution *ex post*. Given the

<sup>23</sup>A *brute* method to implement LCG in parallel is just running independent generators with different seed tables on different processors.

optimal exercise boundary, it is then straightforward to compute the probability of early exercise and the option expected lifetime as functions of time and current state.

This allows us to examine, in the first time, how the stochastic volatility affects the optimal exercise policy of American options. More precisely, we investigate the links between the exercise boundary and the shape of the risk neutral distribution of the underlying asset. In the second time, we study the optimal stopping time problems of American BestOf/WorstOf options.

### 3.1 Optimal exercise boundary: general setting

We make the standard assumptions<sup>24</sup>. The price of an American option  $U^A(t)$  is completely determined by the vector  $X(t)$  of the  $M$  state variables. We have  $U^A(t) = U^A(t, X(t))$ . The risk-free interest rate  $r(t) \geq 0$  is deterministic. For the notational simplicity, we will assume it constant. The exercise of an American option at time  $\tau$  procures for the holder a payoff  $\varrho(\tau, X(\tau))$ . The payoff function  $g$  is continuous and nonnegative. The option is issued at time  $t_0 = 0$ , and the expiration date is  $T$ . The no arbitrage argument imply that the price of an American option verifies

$$U^A(t, X) \geq \varrho(t, X) \quad (39)$$

at each time  $t$ . The stopping region is therefore defined as

$$\mathcal{D} = \{(t, X) \in [0, T] \times \mathcal{R}_X \mid U^A(t, X) = \varrho(t, X)\} \quad (40)$$

The continuation region is the complement of  $\mathcal{D}$  in  $[0, T] \times \mathcal{R}_X$

$$\mathcal{C} = \{(t, X) \in [0, T] \times \mathcal{R}_X \mid U^A(t, X) > \varrho(t, X)\} \quad (41)$$

The stopping boundary is the frontier  $\partial\mathcal{C} \subset \mathcal{D}$  of  $\mathcal{C}$  expressed in terms of the state vector. More formally, we define the critical state as the function  $X^* : [0, T] \rightarrow \mathcal{R}_X$  by setting  $X^*(t) = \{X \in \mathcal{R}_X \mid (t, X) \in \partial\mathcal{C}\}$ . It is sometimes convenient to express the frontier of  $\mathcal{C}$  in terms of one state variable, for example the underlying asset price only in the case of stochastic volatility models. This defines the optimal exercise boundary as the critical price  $S^*$  which is a function of time  $t$  and of the  $M - 1$  remaining state variables. The optimal stopping time is the first time the state vector reaches the stopping boundary. It is thus defined by

$$\begin{aligned} \tau^* &= \inf \{\tau \in [t, T] \mid U^A(\tau, X(\tau)) = \varrho(\tau, X(\tau))\} \\ &= \inf \{\tau \in [t, T] \mid (\tau, X(\tau)) \in \mathcal{D}\} \end{aligned} \quad (42)$$

We note  $Q_T(u; t, X(t))$  the time  $t$  probability of an American option  $U^A$  with maturity  $T \geq t$  to be exercised before time  $u \in [t, T]$ . It is defined as the probability that  $X$  leaves the continuation region before time  $u$ . We have  $Q_T(u; t, X(t)) = \Pr\{\tau^* < u \mid \mathcal{F}_t\}$ . This probability depends on the current time and position as well as of the residual maturity of the option. Taking  $u = T$  we define the probability of premature exercise of the option as

$$Q(t, X(t)) = Q_T(T; t, X(t)) = \Pr\{\tau^* < T \mid \mathcal{F}_t\} \quad (43)$$

This is the probability that  $X$  leaves the continuation region before expiration time  $T$ .

In order to define the expected residual lifetime of an American option, we have to distinguish between two possible events. The first is the event that the option is exercised before expiration time, which occurs with a probability  $Q(t, X(t))$ . The second is the event that the option expires alive, which occurs with a probability  $[1 - Q(t, X(t))]$ . Consequently, the expected residual lifetime verifies

$$\mathfrak{T}(t, X(t)) = E(u \mid u < T) Q(t, X(t)) + (T - t)[1 - Q(t, X(t))] \quad (44)$$

with

$$E(u \mid u < T) = \int_t^T u dQ_T(u; t, X(t)) - t \quad (45)$$

---

<sup>24</sup>In particular, the market permits continuous and frictionless trading and no arbitrage opportunities exist.

It is a function of time  $t$  and of the current state  $X(t)$ .

Let  $\lambda(t) = \lambda(t, X)$  denote the  $N$ -dimensional process of market prices of risk relative to the components of  $W(t)$ . Under suitable regularity conditions, the price of an American option satisfies the variational inequality

$$\begin{cases} \max \{g(t, X) - U^A(t, X), \mathcal{A}^* U^A(t, X) + U_t^A(t, X) - rU^A(t, X)\} = 0 \\ U^A(T, X) = g(T, X) \end{cases} \quad (46)$$

for any  $(t, X) \in [0, T] \times \mathcal{R}_X$  and with  $\mathcal{A}^*$  defined by

$$\mathcal{A}^* f = [\mu(t, X) - \Sigma(t, X) \lambda(t, X)]^\top f_X + \frac{1}{2} \text{trace} \left[ \Sigma(t, X) f_{XX} \Sigma(t, X)^\top \rho \right] \quad (47)$$

In contrast to the free boundary formulation, the variational inequality approach allows us to treat the domain of the American option as an entire region. The optimal boundary can then be recovered from the solution *ex post*. Given the optimal exercise boundary, it is then straightforward to compute the probability of early exercise and the option expected lifetime as functions of  $t$  and  $X$ .

The probability of early exercise  $Q(t, X(t))$  of an American option  $U^A$  is showed to be the solution of the following parabolic partial differential equation (SCHUSS [1980], WILMOTT, DEWYNNE and HOWISON [1993])

$$Q_t(t, X) + \mathcal{A}Q(t, X) = 0 \quad (48)$$

with the boundary conditions

$$\begin{cases} Q(T, X) = 0 & \forall X \in \mathcal{R}_X & (i) \\ Q(t, X) = 1 & \forall (t, X) \in D & (ii) \end{cases} \quad (49)$$

and where  $\mathcal{A}$  is defined by  $\mathcal{A}f = \mu(t, X)^\top f_X + \frac{1}{2} \text{trace} \left[ \Sigma(t, X) f_{XX} \Sigma(t, X)^\top \rho \right]$ . The terminal condition (i) means that when  $t = T$  there is no time left for the state vector to exit from the continuation region. The condition (ii) means that out of the continuation region the probability of leave the continuation region before the maturity is of course 1.

The expected residual lifetime  $\mathfrak{T}(t, X(t))$  of an American option  $U^A$  is showed to satisfy the following partial differential equation

$$\mathfrak{T}_t(t, X) + \mathcal{A}\mathfrak{T}(t, X) = -1 \quad (50)$$

with the boundary conditions

$$\begin{cases} \mathfrak{T}(T, X) = 0 & \forall X \in \mathcal{R}_X & (iii) \\ \mathfrak{T}(T, X) = 1 & \forall (t, X) \in D & (iv) \end{cases} \quad (51)$$

At the maturity time  $T$ , the residual lifetime of an American option is zero, which explains the terminal condition (iii). The condition (iv) means that when  $X$  leaves the continuation region, the option is exercised immediately and its expected residual lifetime vanishes.

### 3.2 American options in SV framework

Stochastic volatility models were introduced in the financial literature by HULL and WHITE [1987], SCOTT [1987] and WIGGINS [1987]. The idea is to generalize the Black and Scholes model by allowing the underlying asset price's volatility itself to be varying. Typically, in a continuous-time framework, volatility is assumed to follow a diffusion process. Standard stochastic volatility models impose  $M = 2$  and  $N = 2$ . Several extensions and special cases can be obtained by varying the number of state variables and sources of randomness.

### 3.2.1 Standard stochastic volatility model

In a standard stochastic volatility model, the state vector is two-dimensional and corresponds to  $X(t) = [S(t) \ V(t)]^\top$ , where  $S(t)$  denotes the underlying asset's price and  $V(t)$  is an extra state variable directly related to the underlying asset returns volatility process. The state diffusion is then

$$\begin{bmatrix} dS(t) \\ dV(t) \end{bmatrix} = \begin{bmatrix} \mu_S(t, S(t), V(t)) S(t) \\ \mu_V(t, V(t)) \end{bmatrix} dt + \begin{bmatrix} \sigma(V(t)) S(t) & 0 \\ 0 & \sigma_V(t, V(t)) \end{bmatrix} \begin{bmatrix} dW_1(t) \\ dW_2(t) \end{bmatrix} \quad (52)$$

where  $W(t) = [W_1(t) \ W_2(t)]^\top$  is a bivariate Wiener process, defined on the fundamental probability space  $(\Omega, \mathcal{F}, \mathbb{P})$ , with  $E[W_1(t)W_2(t)] = \rho(t, V(t))t$ . We note  $\mathbb{F} = \{\mathcal{F}_t, t \in [0, T]\}$  the filtration generated by  $W(t) = [W_1(t) \ W_2(t)]^\top$ . The volatility  $\sigma(t)$ , defined as the instantaneous standard deviation of the underlying asset returns, is a function of the second state variable  $V(t)$ :  $\sigma(t) = \sigma(V(t))$ ,  $t \in [0, T]$ . The function  $\sigma: \mathbb{R} \rightarrow \mathbb{R}_+$  is non-decreasing, Lipschitz and of class  $C^1$ . Moreover, we assume that the underlying asset pays a continuous dividend at a constant rate  $d$ .

Because there is no asset that is clearly instantaneously perfectly correlated with the state variable  $V$ , the market composed of the underlying asset  $S$  and the nonrisky asset  $B$  is not complete. Consequently, the arbitrage arguments are insufficient to determine *uniquely* a probability measure  $\mathbb{Q}$  equivalent to  $\mathbb{P}$ , under which the properly discounted asset prices become martingales (HARRISON and PLISKA [1981, 1983]). Let  $\lambda(t) = [\lambda_1(t) \ \lambda_2(t)]^\top$  be a vector of prices of risk relative to two sources of uncertainty  $W_1(t)$  and  $W_2(t)$ . We obtain

$$\lambda_1(t) = \frac{\mu_S(t, S, V) - r + d}{\sigma(V)} \quad (53)$$

On the other hand, it is not possible to determine the price of risk relative to the stochastic character of the volatility without a general equilibrium model clearly specifying the investors' preferences. For any choice of the price of risk process  $\lambda_2(t)$ , there exists an equivalent martingale measure  $\mathbb{Q}(\lambda_2)$  defined by

$$\frac{d\mathbb{Q}(\lambda_2)}{d\mathbb{P}} = \exp\left(-\int_{t_0}^t \lambda_1(u) dW_1(u) - \frac{1}{2} \int_{t_0}^t \lambda_1^2(u) du - \int_{t_0}^t \lambda_2(u) dW_2(u) - \frac{1}{2} \int_{t_0}^t \lambda_2^2(u) du\right) \quad (54)$$

provided that the Novikov conditions  $\mathbb{E}\left[\exp\frac{1}{2}\int_{t_0}^t \lambda_i^2(u) du\right] < +\infty$ ,  $i = 1, 2$  are satisfied. ROMANO and TOUZI [1996] show that for any risk premium process  $\lambda_2(t)$  satisfying

$$\lambda_2(t) = \lambda(t, V(t)) \quad (55)$$

any European call option completes the market in the sense that the European option hedging problem is solved by a continuously rebalanced delta-sigma strategy. Therefore, as stated in TOUZI [1999], assuming that some European option is traded on the market additionally to the underlying risky asset and the riskless one, permits to extend the arbitrage arguments of BENSOUSSAN [1984] and KARATZAS [1988] and to justify the American option valuation formula

$$U_{\lambda_2}^A(t, S(t), V(t)) = \operatorname{ess\,sup}_{\tau \in \mathcal{T}_{[t, T]}} \mathbb{E}_{\mathbb{Q}(\lambda_2)} \left[ e^{-r(\tau-t)} g(\tau, S(\tau), V(\tau)) \mid \mathcal{F}_t \right] \quad (56)$$

where  $\mathcal{T}_{[t, T]}$  is the set of all stopping times of the filtration  $\mathbb{F}$  with values in  $[t, T]$ <sup>25</sup>. The valuation formula (56) means that for any specification of the risk premium process  $\lambda_2(t)$  satisfying the Novikov condition and the assumption (55),  $U_{\lambda_2}^A(t, S(t), V(t))$  is an admissible American option's price process. Thus, in a standard stochastic volatility model, the price of an American option satisfy the variational inequality (46) with

$$\begin{aligned} \mu(t, X) &= \begin{bmatrix} \mu_S(t, S(t), V(t)) S(t) \\ \mu_V(t, V(t)) \end{bmatrix}, & \Sigma(t, X) &= \begin{bmatrix} \sigma(V(t)) S(t) & 0 \\ 0 & \sigma_V(t, V(t)) \end{bmatrix} \\ \text{and } \lambda(t) &= \begin{bmatrix} \frac{\mu_S(t, S(t), V(t)) - r + d}{\sigma(V(t))} \\ \lambda(t, V(t)) \end{bmatrix} \end{aligned} \quad (57)$$

<sup>25</sup>Given that the filtration  $\mathbb{F}$  corresponds under the assumption (55) to the filtration  $\mathbb{F}^X = \left\{ [S(t) \ V(t)]^\top, t \in [0, T] \right\}$  generated by the vector of state variables, the optimal decision to exercise an American option at time  $\tau$  is based on the observation of the fluctuations of the underlying asset price and its volatility up to time  $\tau$ .

In this standard stochastic volatility setting, the stopping region  $\mathcal{D}$  and the continuation region  $\mathcal{C}$  are defined in three dimensions. The **critical state** corresponds to

$$X^*(t) = \{(S, V) \in \mathcal{R}_X \mid (t, S, V) \in \partial\mathcal{C}\} \quad (58)$$

with  $\mathcal{R}_X \equiv (\mathbb{R}_+^* \cup \{\infty\}) \times (\mathbb{R} \cup \{-\infty, +\infty\})$ . The **critical price** is defined as a function  $S^* : [0, T] \times \mathbb{R} \rightarrow (\mathbb{R}_+^* \cup \{\infty\})$ . Considering the standard American put and call options, we have

$$\begin{cases} \text{Put} & : S^*(t, V) = \sup \{S \in \mathbb{R}_+^* \cup \{\infty\} \mid U_{\lambda_2}^A(t, S, V) = \max(K - S, 0)\} \\ \text{Call} & : S^*(t, V) = \inf \{S \in \mathbb{R}_+^* \cup \{\infty\} \mid U_{\lambda_2}^A(t, S, V) = \max(S - K, 0)\} \end{cases} \quad (59)$$

with standard conventions  $\inf \emptyset = \infty$  and  $\sup \emptyset = 0$ . It is convenient to define the **optimal exercise boundary** as the function  $\vartheta : [0, T] \times \mathbb{R} \rightarrow (\mathbb{R}_+^* \cup \{\infty\})$  given by the equality

$$\vartheta(T - t, V) = S^*(t, V) \quad (60)$$

The optimal exercise boundary can be recovered from the solution of (46). Before applying the numerical FD algorithm, we have to reformulate (46) in terms of  $\tau = T - t$  as an initial value problem. Then, for convenient computation, we have to specify the region  $\mathfrak{R} = [S^-, S^+] \times [V^-, V^+]$  and impose conditions controlling the behavior of  $U^A(\tau, S, V)$  at the boundary of  $\mathfrak{R}$ . Typically one uses the mixed conditions on the  $S$  variable and the usual Neumann conditions for the  $V$  variable. Given the choice of mesh spacings in the time and space directions,  $k$ ,  $h_S$  and  $h_V$  respectively, the problem in (46) is then solved by the *hopscotch* method in the same manner as a standard linear parabolic equation, where at each iteration  $m$ , the solution  $u_{i,j}^{m+1}$  is replaced by

$$\max(u_{i,j}^{m+1}, g(\tau_m, S_i, V_j)) \quad (61)$$

Appropriate coding of this operation permits us to recover *ex post* the optimal exercise boundary  $\vartheta(\tau_m, V_j)$  corresponding to the solution process  $u_{i,j}^{m+1}$ . For any  $m \in \{1, \dots, 1 + \frac{\tau^+}{k}\}$  and  $j \in \{1, \dots, 1 + \frac{V^+ - V^-}{h_V}\}$ , we have

$$\begin{cases} \text{Put} & : \vartheta(\tau_m, V_j) = \inf \{S_i \in \{S^-, \dots, S^+\}, u_{i,j}^{m+1} = f(\tau_m, S_i, V_j)\} \\ \text{Call} & : \vartheta(\tau_m, V_j) = \sup \{S_i \in \{S^-, \dots, S^+\}, u_{i,j}^{m+1} = f(\tau_m, S_i, V_j)\} \end{cases} \quad (62)$$

Given the optimal exercise boundary  $\vartheta(\tau_m, V_j)$ , it is then straightforward to compute the probability of early exercise and the option expected lifetime. Although, the Monte Carlo approach is possible, the finite difference methods applied to the problems (48) and (50) procure us at once the probability of early exercise and the option expected lifetime as functions of  $t$ ,  $S$  and  $V$ .

After reformulating (48) and (50) in terms of  $\tau = T - t$ , the specification of the conditions on the  $S$  variable is in the case of a call option

$$\begin{cases} Q(\tau, S^-, V) = 0 \\ Q(\tau, S^+, V) = 1 \end{cases} \quad \text{and} \quad \begin{cases} \mathfrak{T}_S(\tau, S^-, V) = 0 \\ \mathfrak{T}(\tau, S^+, V) = 0 \end{cases} \quad (63)$$

and in the case of a put option

$$\begin{cases} Q(\tau, S^-, V) = 1 \\ Q(\tau, S^+, V) = 0 \end{cases} \quad \text{and} \quad \begin{cases} \mathfrak{T}(\tau, S^-, V) = 0 \\ \mathfrak{T}_S(\tau, S^+, V) = 0 \end{cases} \quad (64)$$

For the  $V$  variable, a general approach is to impose standard Neumann conditions. Given the choice of mesh spacings and given  $\vartheta(\tau_m, V_j)$ , the problems are solved by the *hopscotch* method in the same manner as standard linear parabolic equations, but with the solutions  $Q_{i,j}^{m+1}$  and  $\mathfrak{T}_{i,j}^{m+1}$  constrained to satisfy for any  $m$ ,  $i$  and  $j$ ,  $Q_{i,j}^{m+1} = 1$  if  $S_i \geq \vartheta(\tau_m, V_j)$  and  $\mathfrak{T}_{i,j}^{m+1} = 0$  if  $S_i \geq \vartheta(\tau_m, V_j)$  in the case of a call, and  $Q_{i,j}^{m+1} = 1$  if  $S_i \leq \vartheta(\tau_m, V_j)$  and  $\mathfrak{T}_{i,j}^{m+1} = 0$  if  $S_i \leq \vartheta(\tau_m, V_j)$  in the case of a put.

### 3.2.2 Optimal exercise boundary in Heston model

In this section, we illustrate how the random behavior of the underlying asset price volatility affects the American option optimal exercise boundary. We adopt the fully parametrized stochastic volatility framework of HESTON [1993]. However, our qualitative results can easily be extended to other specifications of the underlying asset price dynamics.

Different specifications of the state vector dynamics (52) were proposed in the financial literature. Among them, the model of Heston received considerable attention because of the existence of near-analytic solutions to European options valuation formulas (see BAKSHI, CAO and CHEN [1997]). Moreover, all the parameters of the model can be consistently estimated from a time series of the underlying asset price and of one European option price (see CHERNOV and GHYSELS [1999] and KURPIEL [2000] for empirical applications).

Heston defines the state variable  $V(t)$  as the instantaneous variance of the underlying asset returns and assumes that  $V(t)$  follows a square root process. The state diffusion is then

$$\begin{bmatrix} dS(t) \\ dV(t) \end{bmatrix} = \begin{bmatrix} \mu_S S(t) \\ \kappa [\theta - V(t)] \end{bmatrix} dt + \begin{bmatrix} \sqrt{V(t)} S(t) & 0 \\ 0 & \sigma_V \sqrt{V(t)} \end{bmatrix} \begin{bmatrix} dW_1(t) \\ dW_2(t) \end{bmatrix} \quad (65)$$

with  $\mathbb{E}[W_1(t)W_2(t)] = \rho t$ ,  $\kappa > 0$ ,  $\theta > 0$ ,  $\sigma_V > 0$ . Adopting the general CIR equilibrium framework and assuming that investors' utility functions are of CRRA type, Heston derives the following market price of risk process  $\lambda_2(t) = \frac{\lambda}{\sigma_V} \sqrt{V(t)}$ ,  $\lambda \in \mathbb{R}$ . Under the equivalent martingale measure  $\mathbb{Q}(\lambda_2)$ , the state vector dynamics becomes

$$\begin{bmatrix} dS(t) \\ dV(t) \end{bmatrix} = \begin{bmatrix} (r-d)S(t) \\ \kappa^* [\theta^* - V(t)] \end{bmatrix} dt + \begin{bmatrix} \sqrt{V(t)} S(t) & 0 \\ 0 & \sigma_V \sqrt{V(t)} \end{bmatrix} \begin{bmatrix} dW_1^*(t) \\ dW_2^*(t) \end{bmatrix} \quad (66)$$

where by virtue of the Girsanov theorem, the process  $W^*(t) = [W_1^*(t) \ W_2^*(t)]^\top$  defined by  $W_i^*(t) = W_i(t) + \int_0^t \lambda_i(u) du$  ( $i = 1, 2$ ) is a two-dimensional Wiener process under  $\mathbb{Q}(\lambda_2)$ , with  $\mathbb{E}[W_1^*(t)W_2^*(t)] = \rho t$ , and where  $\kappa^* = (\kappa + \lambda)$  and  $\theta^* = \frac{\kappa\theta}{\kappa + \lambda}$ . Given that  $\lambda_2(t)$  satisfies (55), all the regularity results by TOUZI [1999] hold. In particular, the optimal exercise boundary  $\vartheta$ , as defined in (60), is a function of two variables: the time to expiration of the option and the current instantaneous variance of the underlying asset returns. For a given level of the current variance, it is rational to exercise the option at the first time the underlying asset price crosses the optimal exercise boundary.

Figure (13) shows the optimal exercise boundary for an American put with  $K = 100$  in a Heston stochastic volatility model with the following parameter values :  $r = 0.08$ ,  $d = 0$ ,  $\kappa = 0.9$ ,  $\theta = 0.04$ ,  $\lambda = 0$ ,  $\sigma_V = 0.1$  and  $\rho = -0.5$ . We can see that the optimal exercise boundary of an American put is decreasing in time to expiration and in current variance<sup>26</sup>. Symmetrically, provided that the asset pays a positive dividend, the optimal exercise boundary of an American call is increasing in the time to expiration and in the current level of the volatility.

The shape of the optimal exercise boundary depends on the contractual characteristics of the American option and on the shape of the state vector's risk neutral distribution. In a fully parametrized stochastic volatility model, it is therefore interesting to distinguish between four groups of parameters

1. The parameters that determine the first moment of  $S(t)$  under  $\mathbb{Q}(\lambda_2)$ , i.e. the risk free interest rate  $r$  and the dividend yield  $d$ ;
2. The parameters that affect the average second moment of  $S(t)$ , i.e. the parameters that determine the first moment of  $V(t)$  under  $\mathbb{Q}(\lambda_2)$ ;
3. The parameters that affect the third moment of  $S(t)$ , i.e. the correlation between the underlying asset returns and their volatility;

<sup>26</sup>Touzi [1999] demonstrates rigorously this result in the general standard stochastic volatility framework.

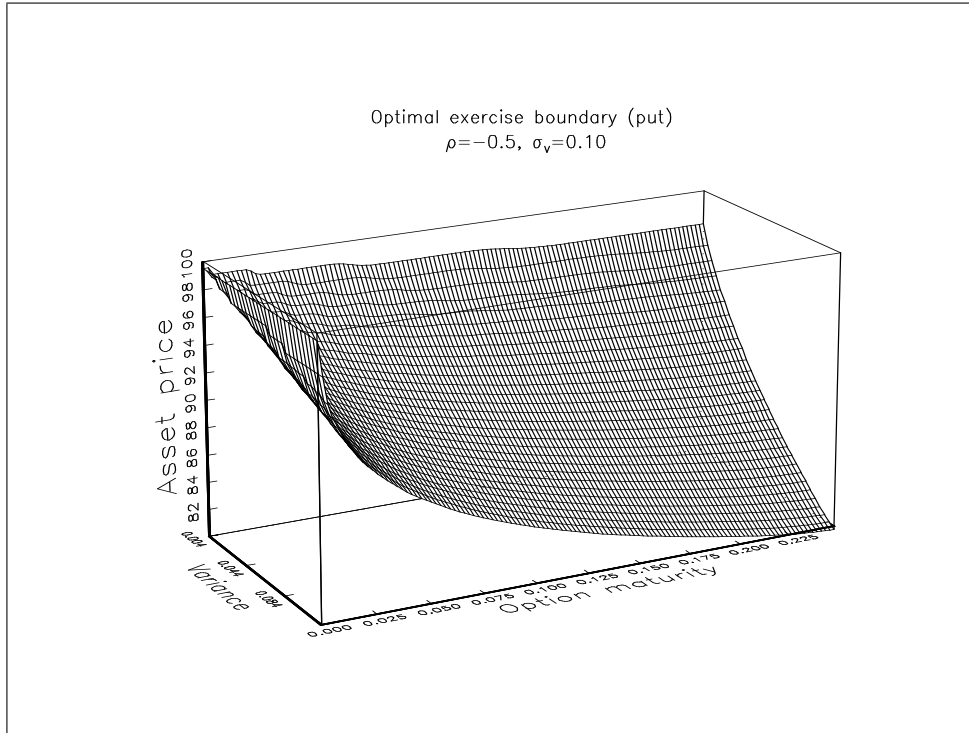


Figure 13: Optimal exercise boundary for an American put

4. The parameters that determine the fourth moment of  $S(t)$ , i.e. the volatility of the volatility.

The qualitative impact on the optimal exercise boundary of the contractual characteristics of the option and of the parameters affecting the first moment of  $S(t)$  is the same in the constant volatility and in the stochastic volatility environments. We refer to MOERBEKE [1976], KIM [1990] and BARLES, BURDEAU, ROMANO and SAMSOEN [1992] for basic properties of the optimal stopping boundary when the underlying asset price is generated by a constant volatility diffusion process. Table 3 resumes the impact on  $\vartheta$  of an increase in exercise price, dividend yield and interest rate, all else remaining unchanged<sup>27</sup>.

Parameter		Call	Put
Exercise price	$K$	+	+
Dividend yield	$d$	-	-
Interest rate	$r$	+	+

Table 3: The impact of parameters on the optimal exercise boundary

An American option is exercised before expiration if the benefits outweigh the cost associated with early exercise. This explains the basic relations presented in table 3. Early exercise of an American put may be interpreted as an exchange of dividends to be received from the asset for interest to be earned on the exercise price. Symmetrically, early exercise of an American call may be interpreted as an exchange of interest to be earned on the exercise price for dividends to be received from the asset. Table 4 resumes the impact on  $\vartheta(T-t, V)$  of an increase in different parameters of the model of Heston, all else remaining unchanged. The impact of  $\theta^*$  and  $\kappa^*$  on the optimal exercise boundary follows from the way they affect the average variance under  $\mathbb{Q}(\lambda_2)$ . When  $\kappa^* > 0$ , i.e.  $\kappa > -\lambda$ , the risk-neutralized instantaneous variance process has a steady-state distribution with mean  $\theta^*$ . Consequently, when  $\theta^*$  gets higher, the long-run mean under  $\mathbb{Q}(\lambda_2)$  of the instantaneous variance increase and the optimal exercise boundary moves away from the exercise price for

<sup>27</sup>A + and a - signify respectively an upward and a downward shift of the optimal boundary, a 0 signifies no impact.

both calls and puts. The impact of  $\kappa^*$  on the conditional mean of the  $V(t)$  under  $\mathbb{Q}(\lambda_2)$  changes according to the position of the current variance with respect to  $\theta^*$ . For the values of the current instantaneous variance greater than  $\theta^*$  (lower than  $\theta^*$ ), an increase of  $\kappa^*$  reduces (increases) the first conditional moment of  $V(t)$ . Thus, for both calls and puts, a greater mean-reversion speed  $\kappa^*$  makes the optimal exercise surface less steeply inclined in the  $V$  variable, keeping unchanged the central node corresponding to  $V = \theta^*$ . It means that a greater mean-reversion speed  $\kappa^*$  reduces the sensitivity of the optimal exercise boundary with respect to the current variance. The risk premium parameter  $\lambda$  affects the long-run mean and the mean-reversion speed of the instantaneous variance process according to (66). For a lower value of  $\lambda$ , the long-run mean  $\theta^*$  is higher and the mean-reversion speed  $\kappa^*$  is lower, which shifts the optimal exercise boundary away from the exercise price and makes it more sensitive with respect to the current volatility changes.

Parameter	Call	Put	
$\theta^*$	+	-	
$\lambda$	-	+	
$\rho$	-	-	
$\kappa^*$	$V < \theta^*$	+	-
	$V = \theta^*$	0	0
	$V > \theta^*$	-	+
$\sigma_V$	$\rho < 0$	+	+
	$\rho = 0$	+	-
	$\rho > 0$	-	-

Table 4: The impact of parameters on the optimal exercise boundary

The impact of  $\rho$  on the American options optimal exercise boundary, is related to the way the correlation between  $V(t)$  and  $S(t)$  affects the shape of the distribution of  $S(u)$ ,  $u > t$ . The parameter  $\rho$  being significantly different from zero induces an asymmetry on the conditional distribution of  $S(u)$ . A negative (positive) correlation between the asset returns and their volatility corresponds to a negatively (positively) skewed distribution of futures asset prices. Assymetries in the distribution of futures asset prices are consistent with asymmetries in the European options implied volatility smiles. Typical patterns of implied volatility smiles suggest  $\rho < 0$  for stocks and stock indexes,  $\rho \simeq 0$  for exchange rates and  $\rho > 0$  for some commodities. Figure<sup>28</sup> (14) shows the impact of  $\rho$  on the optimal exercise boundary for an American put with the exercise price  $K = 100$ .

One may regret early exercise of an American put if the underlying asset price increases substantially later on. But the probability of a substantial increase in  $S(t)$  is relatively lower when  $\rho < 0$ . Consequently, an unfavorable scenario following the early exercise of an American put is less likely when the underlying asset returns are negatively correlated with their volatility. This explains why, for each  $t$ , the optimal exercise boundary of an American put is nearer to the exercise price  $K$  when  $\rho < 0$  compared to the case of  $\rho \geq 0$ . On the other hand, one may regret early exercise of an American call if the underlying asset price decreases substantially later on. When  $\rho < 0$ , the probability that  $S(t)$  falls substantially is greater than in the case of  $\rho \geq 0$ . Thus, when the correlation between the underlying asset returns and their volatility is negative, it is optimal to exercise an American call at a greater critical price compared to the case of the positive or zero correlation.

The volatility of the instantaneous variance, measured in the model of Heston by the parameter  $\sigma_V$ , influences the tails of the conditional distribution of the underlying asset price. The greater is  $\sigma_V$ , the more fat tailed is the distribution of  $S(u)$ . Consequently, when  $\rho$  is significantly different from zero,  $\sigma_V$  reinforces the impact of  $\rho$  on the optimal exercise surface. When  $S(t)$  is not correlated with  $V(t)$ , the impact of  $\sigma_V$  on the optimal exercise boundary may be viewed as the impact of the random behavior *per se* of the volatility. Figure (15) shows the impact of  $\sigma_V$  on the optimal exercise boundary for an American put with the exercise price  $K = 100$ .

<sup>28</sup>In order to make our graphical representations clear, we present only the central part of the optimal exercise boundary, with  $V(t) = \theta^*$ ,  $\forall t \in [0, T]$ . Figures (14) and (15) shows the optimal exercise boundaries of American puts in the model of Heston with  $\theta = 0.04$ ,  $\kappa = 0.9$ ,  $\lambda = 0$ ,  $r = 0.08$  and  $d = 0$ .

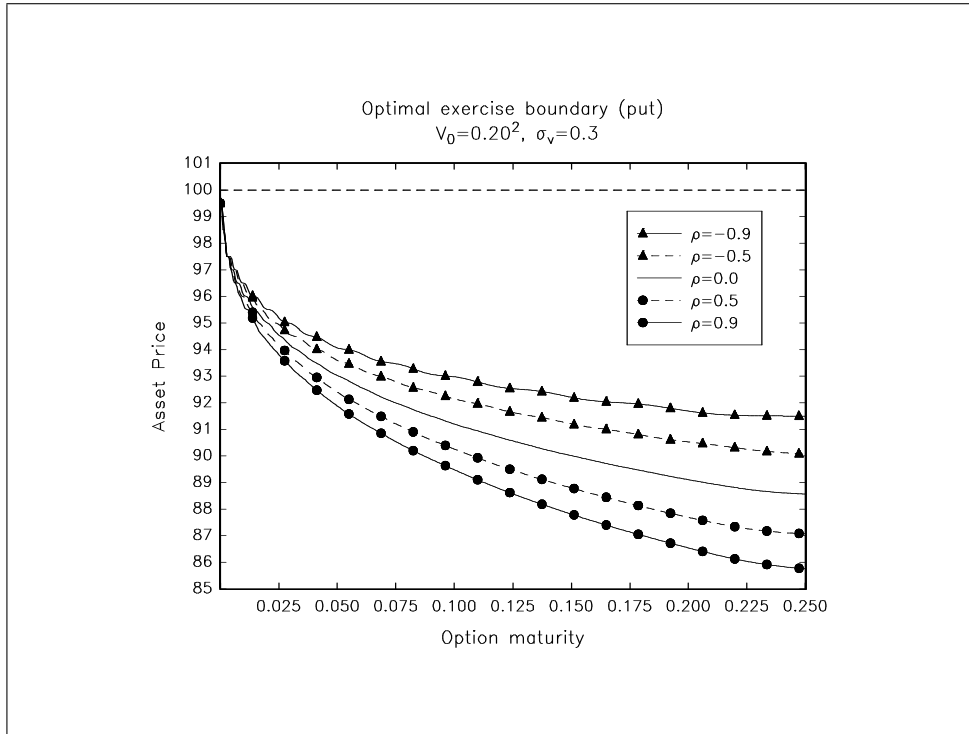


Figure 14: Influence of the  $\rho$  parameter on the optimal exercise boundary for an American put

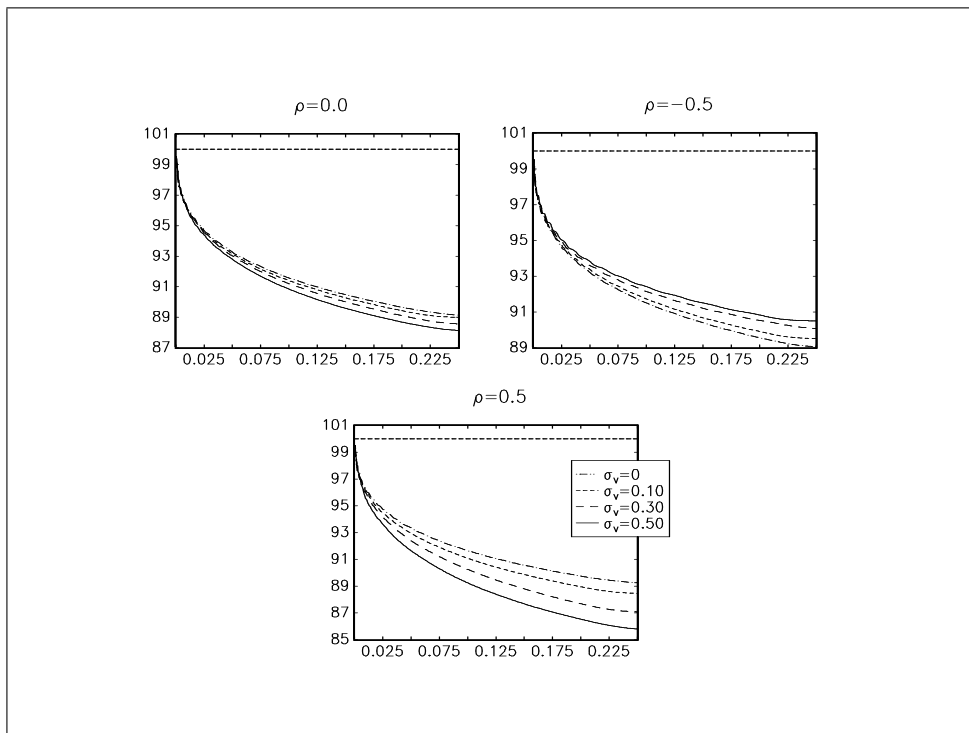


Figure 15: Influence of the  $\sigma_V$  parameter on the optimal exercise boundary for an American put

In the case of an American put, when  $\rho < 0$ , the probability that an unfavorable scenario occurs after the early exercise of the option is all the lower as  $\sigma_V$  is higher, which explains the upward shift of the optimal exercise boundary. In the case of an American call, when  $\rho < 0$ , the probability that the underlying asset price falls substantially after the early exercise of the option is all the higher as  $\sigma_V$  is greater. Consequently, the optimal exercise boundary of the American call on an asset with high volatile returns variability is located at a greater distance from the exercise price  $K$ . When the underlying asset returns are not correlated with their instantaneous variance ( $\rho = 0$ ), a greater  $\sigma_V$  implies a higher probability of an extreme event (such as a strong increase or a strong decrease of the underlying asset price after the early exercise of the option). Consequently, the optimal exercise surface for both American calls and puts is located further from the exercise price  $K$  when the variability of the underlying asset returns is more volatile.

Figure (15) presents also the case of  $\sigma_V = 0$  which corresponds to the constant volatility model. For that case, the optimal exercise boundary was computed using the implied volatility at time  $t_0$  obtained from the “market” prices of **at-the-money** options<sup>29</sup> given by the Heston stochastic volatility model with  $\sigma_V = 0.3$ . In this way, we can visualize the general impact of the random behavior of volatility on the optimal exercise boundary and observe the biases generated by the constant volatility model when one uses it in a stochastic volatility environment.

Applying a standard constant volatility model is equivalent to assuming a log-normal conditional distribution for  $S(u)$ ,  $u > t$ . When the volatility of the underlying asset returns is stochastic ( $\sigma_V \neq 0$ ), the conditional distribution of  $S(u)$  has fat tails. Moreover, this distribution is skewed if  $\rho \neq 0$ . Consequently, in the case of an American put, the use of the constant volatility model in a stochastic volatility environment produces critical prices that are, for a given level of the current volatility, too distant from the exercise price  $K$  if  $\rho < 0$ , i.e. exercise rule is too stringent, and that are too close to the exercise price  $K$  if  $\rho \geq 0$ , i.e. the exercise rule is too loose. In the case of an American call, assuming wrongly that the volatility is constant, will lead to the critical prices located too far from  $K$  if  $\rho > 0$  and too close to  $K$  if  $\rho \leq 0$ .

### 3.3 American options with two-underlying assets

Multi-asset options market has been increasingly developing for some months. It enables to speculate or to hedge against correlation moves. We present here an application of the *Hopscotch* method for the pricing of the two asset options. This paragraph will focus on the standard following payoffs

$$\begin{aligned} \text{BestOf} & \quad \max \left[ \max \left[ \alpha_1 \left( \frac{S_1(T)}{S_1(t_0)} - K_1 \right), \alpha_2 \left( \frac{S_2(T)}{S_2(t_0)} - K_2 \right) \right], 0 \right] \\ \text{WorstOf} & \quad \max \left[ \min \left[ \alpha_1 \left( \frac{S_1(T)}{S_1(t_0)} - K_1 \right), \alpha_2 \left( \frac{S_2(T)}{S_2(t_0)} - K_2 \right) \right], 0 \right] \end{aligned} \quad (67)$$

where  $\alpha_1$  and  $\alpha_2$  are equal to 1 or -1, so that we will be interested by the best (or the worst) of two Call, two Put, or one Call and one Put.

The European case is trivial since there is a quasi explicit formula to price such options. For instance, if  $K_1 = K_2 = K$ , the price of a BestOf Call/Call may be given by

$$\begin{aligned} C(t_0) & = e^{-r(T-t_0)} \mathbb{E}_{\mathbb{Q}} \left( \max \left[ \left( \frac{S_1(T)}{S_1(t_0)} - K \right)^+, \left( \frac{S_2(T)}{S_2(t_0)} - K \right)^+ \right] \mid \mathcal{F}_0 \right) \\ & = e^{-r(T-t_0)} \int_K^{+\infty} (1 - G(x)) dx \end{aligned} \quad (68)$$

where  $G$  is the cumulative distribution function of  $\max \left( \frac{S_1(T)}{S_1(t_0)}, \frac{S_2(T)}{S_2(t_0)} \right)$

$$G(x) = \int_{-\infty}^{+\infty} \prod_{i=1}^2 \Phi \left( \frac{\ln(x) + \left( r + \frac{\sigma_i^2}{2} \right) (T - t_0)}{\sigma_i \sqrt{T - t_0} \sqrt{1 - \rho^2}} - \frac{\rho z}{\sqrt{1 - \rho^2}} \right) d\Phi(z) \quad (69)$$

<sup>29</sup>In a stochastic volatility environment, the Black and Scholes implied volatility is a function of the current state. Consequently, the magnitude and the sign of the exercise boundary bias is affected by the current underlying asset price, see KURPIEL [1999] for further investigations in this direction.

Those integrals will be computed in the following using a Gauss-Hermite quadrature and will enable us to check the adequacy of our boundary conditions and the accuracy of our mesh when pricing with Hopscotch method.

In this standard model, the state vector is obvious and the market is complete. Any option payoff may be replicate using delta hedging strategy. Once again, the price of an American option written on these two underlyings satisfies a two-dimensional variational inequality. We may then extract the optimal exercise boundary from the solution. It is not useful to compute every American prices. Indeed, like in the single underlying context, some American option prices are equal to their european prices. For instance, it is not difficult to show that the BestOf Call/Call American component price is equal to zero, since the price process is a sub-martingale<sup>30</sup>. This property does not hold anymore for the price of BestOf Put/Put options. In this case, it is more difficult to compute the American prime and to describe the optimal exercise boundary. Then, numerical procedures to solve this kind of problem are usually based on trees and PDE. As already mentionned, our American price  $U^A(t, S_1(t), S_2(t))$  is the solution of the variational inequality (46). To solve it numerically, we need to limit  $(S_1, S_2)$  to  $\mathfrak{R} = [S_1^-, S_1^+] \times [S_2^-, S_2^+]$  and to impose some boundary conditions. In this case we will mix Dirichlet and Neumann conditions. Indeed, we have imposed

$$\begin{cases} \frac{\partial U^A(t, S_1^-, S_2)}{\partial S_1} = \frac{\partial U^A(t, S_1, S_2^-)}{\partial S_2} = -1 \\ U^A(t, S_1^+, S_2) = (K_2 - S_2)^+ \\ U^A(t, S_1, S_2^+) = (K_1 - S_1)^+ \end{cases} \quad (70)$$

In order to check the adequacy of these conditions and the accuracy of the mesh, we have compared prices obtained using *Hopscotch* in the European case to the quasi-analytic expression. Tests have been carried out pricing a one month BestOf Put/Put<sup>31</sup> with a mesh fixed to  $N_t = 250$  and  $N_x = N_x = 360$ . Errors observed are inferior to  $10^{-5}\%$ ! We represent in the figure 17 the optimal exercise boundary of such an option. This figures points out 2 important facts:

- There is a non negligible set where it is optimal to exercise for the holder. **It means that the american component price may play an important role in the price of such an option.**
- **The optimal exercise set of the BestOf Put/Put is smaller than the union of the two optimal exercise set of the single american puts.** In other words, one may observe that when the two underlyings decrease so that they may both cross their optimal exercise boundary, it is not always optimal to exercise the two-assets option. It may be worth waiting to know which Put will be more interesting.

One may remark that for a given  $S_2$  the projection of this optimal exercise boundary is varying with time in the same way as the usual single american put exercise boundary does. Finally, An illustration of the relative difference<sup>32</sup> between the European and American prices is represented in the figure 16.

## 4 Some hedging problems

### 4.1 Managing the smile effect

#### 4.1.1 General issue and approximation

It is not an easy task to measure effects of the so-called volatility smile on such financial products. Indeed, information available in the market deals with vanilla options written on a single underlying, and even in this simple case there is no general agreement to modelize this effect. Thus, the choice of the “fair” volatility for multi-asset options may not be obvious. Professionals who think in a Black-Scholes framework have then to look for some rules of pricing. Nevertheless, these rules are based on proxies and there is always some

<sup>30</sup>in the case  $b_1 = b_2 = r$ .

<sup>31</sup>The parameters are  $b_1 = b_2 = r = 5\%$ ,  $\sigma_1 = \sigma_2 = 15\%$ ,  $\rho = \frac{1}{2}$ ,  $T - t_0 = \frac{1}{12}$  and  $K_0 = K_1 = 1$ .

<sup>32</sup>The results are very sensible to the parameters. For example, with the parameters  $b_1 = 2.5\%$ ,  $\sigma_1 = 15\%$ ,  $b_2 = 7.5\%$ ,  $\sigma_2 = 25\%$ ,  $\rho = -\frac{1}{2}$ ,  $T - t_0 = \frac{3}{12}$ ,  $r = 5\%$ ,  $K_1 = 1$  and  $K_2 = 1.1$ , we obtain the figures 18 and 19.

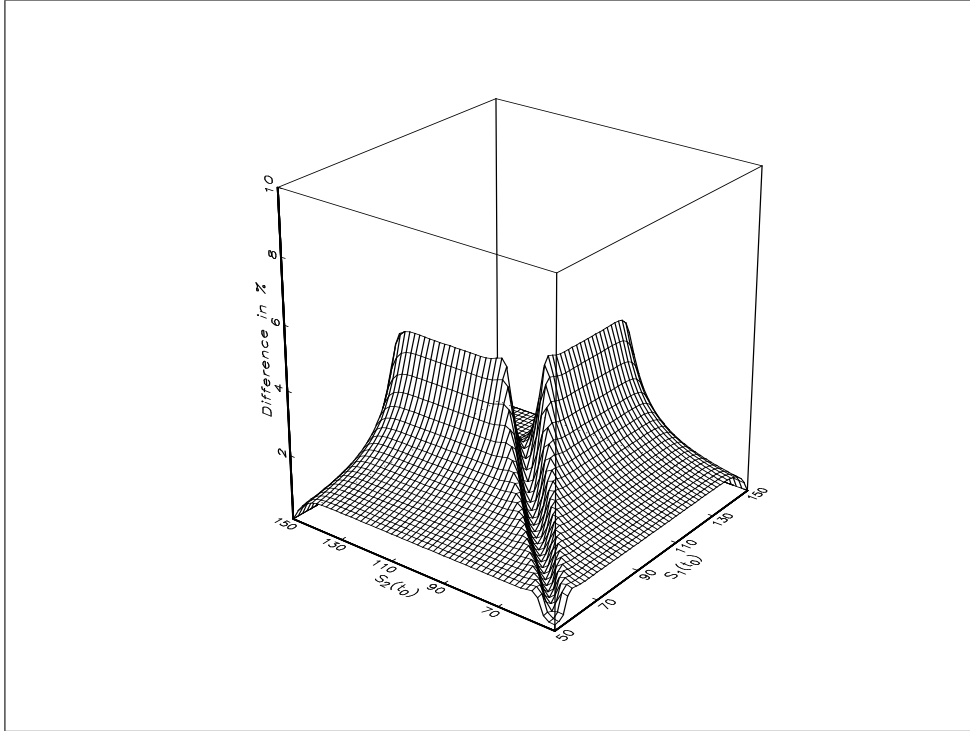


Figure 16: American price of a BestOf Put/Put option vs European price (I)

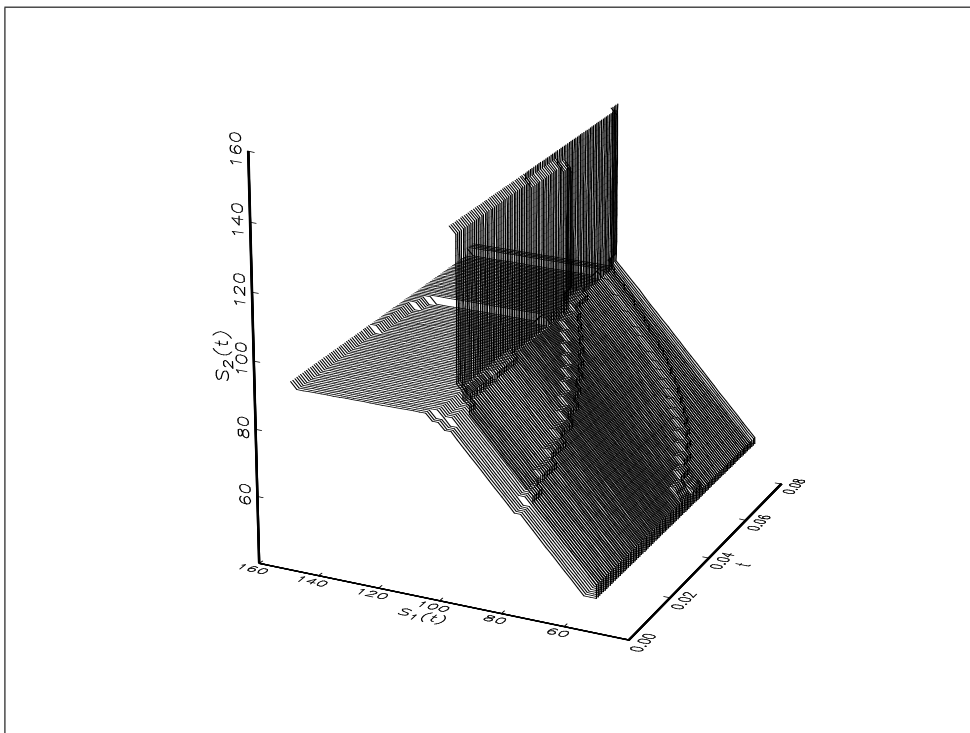


Figure 17: Optimal exercise policy of the American BestOf Put/Put option (I)

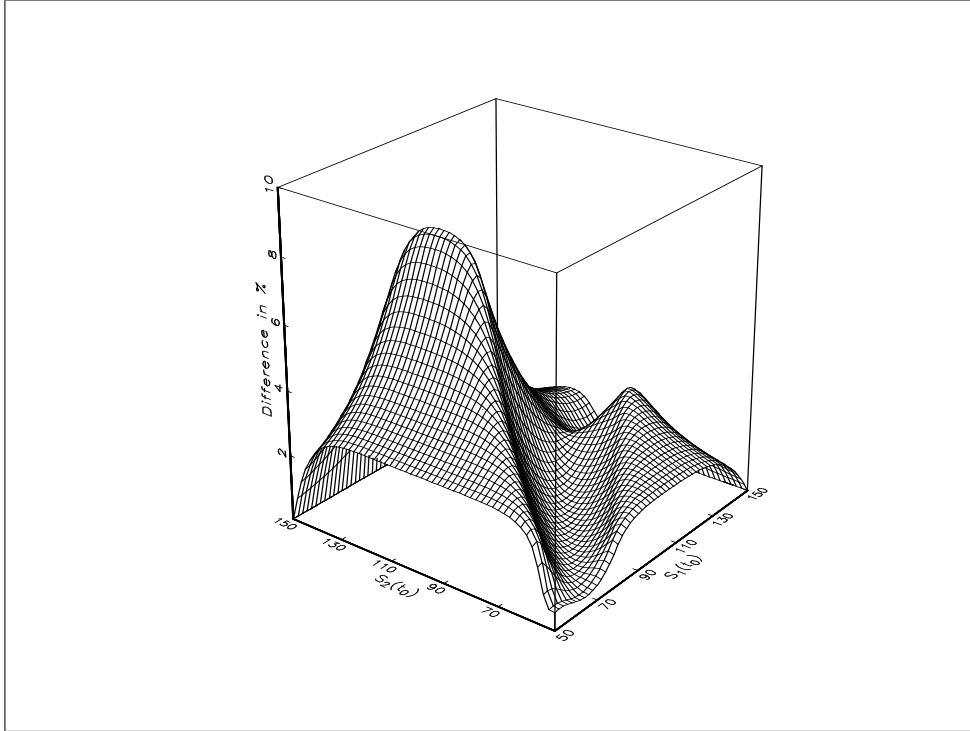


Figure 18: American price of a BestOf Put/Put option vs European price (II)

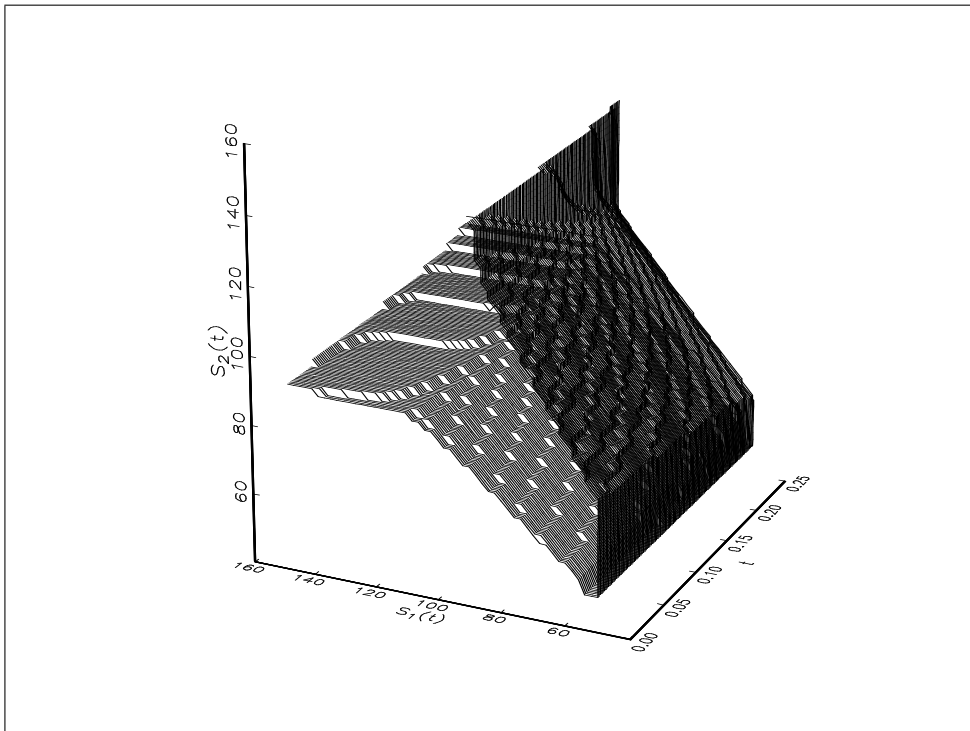


Figure 19: Optimal exercise policy of the American BestOf Put/Put option (II)

residual errors. Moreover, these rules are far from being always obvious. Indeed, consider a spread option whose payoff is  $(S_1(T) - S_2(T))^+$  where  $S_1(t)$  and  $S_2(t)$  follow a stochastic volatility model (for example the Heston model), and try to guess which volatility we may have to input in a Black-Scholes pricer to get the fair price. A natural approach may be to choose the at-the-money volatility for both assets. Monte-Carlo simulations will show that this approach leads to relative errors about 15% for a quite pronounced smile<sup>33</sup>. In practice, these residual errors are then compensated by the choice of a suitable correlation and depend on traders' skills.

Let us remark that it is very difficult to calibrate a multi-asset stochastic volatility model. Indeed, it needs to estimate a lot of parameters whose some are not likely to be relevant with both option and asset prices. It actually leads to high unstablity of these parameters. Nevertheless, some proxies enable to incorporate volatility smile into a quasi-analytical price of a spread option. A simple approach may be to consider that the volatility risk does not affect the probability that  $S_1(T) \geq S_2(T)$ . That is why, one may consider 2 assets:

- $S_1$  whose volatility is stochastic (and follows for example Heston model);
- $\tilde{S}_2$  which follows a classical log-normal diffusion.

So, one has to consider dynamics of  $S_1(t)$  such as

$$\begin{cases} dS_1(t) &= rS_1(t) dt + \sigma_1(t) S_1(t) dW_1(t) \\ dV_1(t) &= \kappa_1(V_1(\infty) - V_1(t)) dt + \sigma_{V_1}\sigma_1(t) d\tilde{W}_1(t) \end{cases} \quad (71)$$

with  $\sigma_1(t) = \sqrt{V_1(t)}$ . Furthermore, we have

$$d\tilde{S}_2(t) = r\tilde{S}_2(t) dt + \sigma_2\tilde{S}_2(t) dW_2(t) \quad (72)$$

We note  $\eta$  the correlation between  $W_1(t)$  and  $\tilde{W}_1(t)$ , and  $\rho$  the correlation between the two asset returns. Then we may introduce an option whose price may be an approximation of the call spread price, that is to say

$$\mathbb{E}_{\mathbb{Q}}\left((S_1(T) - S_2(T))^+ \mid \mathcal{F}_0\right) \simeq \mathbb{E}_{\mathbb{Q}}\left(\left(S_1(T) - \tilde{S}_2(T)\right)^+ \mid \mathcal{F}_0\right) \quad (73)$$

One may decompose  $W_1(t)$  as follows

$$W_1(t) = \rho W_2(t) + \sqrt{1 - \rho^2} W_3(t) \quad (74)$$

where  $W_3(t)$  is a standard Brownian motion independant of  $W_2(t)$ . The diffusion process (71) becomes

$$\begin{cases} dS_1(t) &= rS_1(t) dt + \rho\sigma_1(t) S_1(t) dW_2(t) + \sqrt{1 - \rho^2}\sigma_1(t) S_1(t) dW_3(t) \\ dV_1(t) &= \kappa_1(V_1(\infty) - V_1(t)) dt + \sigma_{V_1}\sigma_1(t) d\tilde{W}_1(t) \end{cases} \quad (75)$$

One may write  $S_1(t)$  as the product of two independant terms, i.e

$$\begin{aligned} S_1(t) &= \underbrace{S_1(t_0) \exp\left(r(t-t_0) - \frac{1-\rho^2}{2} \int_{t_0}^t \sigma_1^2(s) ds + \sqrt{1-\rho^2} \int_{t_0}^t \sigma_1(s) dW_3(s)\right)}_{X_1(t)} \\ &\times \underbrace{\exp\left(-\frac{\rho^2}{2} \int_{t_0}^t \sigma_1^2(s) ds + \rho \int_{t_0}^t \sigma_1(s) dW_2(s)\right)}_{Y_1(t)} \end{aligned} \quad (76)$$

---

<sup>33</sup>By quite pronounced smile, we mean

$$\begin{aligned} \kappa &= 0.5 \\ \sigma_V &= 0.9 \end{aligned}$$

and the correlation between the brownian of the asset and the brownian of the volatility is about  $-0.5$ .

The second term of this last expression enables to get some dependance between the two assets. As mentioned before, one may assume that the effect of stochastic volatility on this dependance is negligible. So we may replace  $\sigma_1(t)$  which is stochastic by a suitable implied volatility  $\hat{\sigma}_1(t)$  (at-the-money volatility for instance) in the second term of  $S_1(t)$ :

$$\begin{aligned} \mathbb{E}_{\mathbb{Q}} \left( \left( S_1(T) - \tilde{S}_2(T) \right)^+ \mid \mathcal{F}_0 \right) &= \mathbb{E}_{\mathbb{Q}} \left( Y_1(T) \underbrace{\mathbb{E}_{\mathbb{Q}} \left( \left( X_1(T) - \frac{\tilde{S}_2(T)}{Y_1(T)} \right)^+ \mid W_2 \right)}_{\text{Call}_{\text{Heston}}(t_0, T, \frac{\tilde{S}_2(T)}{Y_1(T)})} \mid \mathcal{F}_0 \right) \\ &= \int_{-\infty}^{+\infty} \frac{1}{\sqrt{2\pi}} y(x) \text{Call}_{\text{Heston}}(t_0, T, K(x)) \exp\left(-\frac{1}{2}x^2\right) dx \end{aligned} \quad (77)$$

where

$$y(x) \simeq \exp\left(-\frac{1}{2}\rho^2\hat{\sigma}_1^2(T-t_0) + \rho\hat{\sigma}_1x\sqrt{T-t_0}\right) \quad (78)$$

and

$$K(x) \simeq S_2(t_0) \exp\left(r(T-t_0) - \frac{1}{2}(\hat{\sigma}_2^2 - \rho^2\hat{\sigma}_1^2)(T-t_0) + (\hat{\sigma}_2 - \rho\hat{\sigma}_1)x\sqrt{T-t_0}\right) \quad (79)$$

**Remark 1** We may notice that  $\rho$  plays some role in the term  $\text{Call}_{\text{Heston}}(t_0, T, K(x))$ . One may take it into account in a more convenient way, writing the diffusion process of  $X_1(t)$  as follows

$$\begin{cases} dX_1(t) &= rX_1(t) dt + \sigma_X(t) X_1(t) dW_3(t) \\ dV_X(t) &= \kappa_X(V_X(\infty) - V_X(t)) dt + \bar{\sigma}\sigma_X(t) d\tilde{W}_3(t) \end{cases} \quad (80)$$

with  $\sigma_X(t) = \sqrt{1 - \rho^2}\sigma_1(t)$ , so that one get the equivalence

$$\begin{aligned} \kappa_X &= \kappa_1 \\ V_X(\infty) &= (1 - \rho^2)V_1(\infty) \\ \bar{\sigma} &= \sqrt{1 - \rho^2}\sigma_{V_1} \end{aligned} \quad (81)$$

**Remark 2** This approach may be useful when one observes enough vanilla prices on one of both assets in the market, or when smile curve is smooth enough to interpolate missing values. Indeed, one may then replace the integral by a finite sum. Notice that this approach provide us with a natural hedging strategy which consists in buying Vanillas. This hedge enables anyone to take into account volatility risk.

#### 4.1.2 Application to BestOf/WorstOf Call/Put

One may use previous fomula to price other payoffs we are interested in. Indeed, considering that

$$(\max(S_1(T), S_2(T)) - K)^+ = (S_2(T) - K)^+ + (S_1(T) - \max(S_2(T), K))^+ \quad (82)$$

it is possible to use results from the expression (77) so that one can get an approximation of a BestOf Call by

$$\mathbb{E}_{\mathbb{Q}} \left( \left( S_1(T) - \max(\tilde{S}_2(T), K) \right)^+ \mid \mathcal{F}_0 \right) = \int_{-\infty}^{+\infty} \frac{1}{\sqrt{2\pi}} y(x) \text{Call}_{\text{Heston}}(t_0, T, K(x)) \exp\left(-\frac{1}{2}x^2\right) dx \quad (83)$$

with

$$y(x) \simeq \exp\left(-\frac{1}{2}\rho^2\hat{\sigma}_1^2(T-t_0) + \rho\hat{\sigma}_1x\sqrt{T-t_0}\right) \quad (84)$$

and

$$K(x) \simeq y^{-1}(x) \max\left(S_2(t_0) \exp\left(\left(r - \frac{1}{2}\hat{\sigma}_2^2\right)(T-t_0) + \hat{\sigma}_2x\sqrt{T-t_0}\right), K\right) \quad (85)$$

We have implemented this method when the smile is built with 36 Vanilla prices (from strike 70 to strike 140 with a step of 2). The integral is computed following Gauss-Hermite quadrature with 32 nodes. Results and comparisons are presented in the figure 20 for the WorstOf Put/Put option with two different Risk Reversal<sup>34</sup>. The proxy prices have been computed without using Heston formula. Furthermore, prices of Vanilla have not been interpolated, so that these results could be improved. Nevertheless, this approach seems quite interesting for the pricing of these options. They may reduce the few residual errors observed with the B&S pricer for those options.

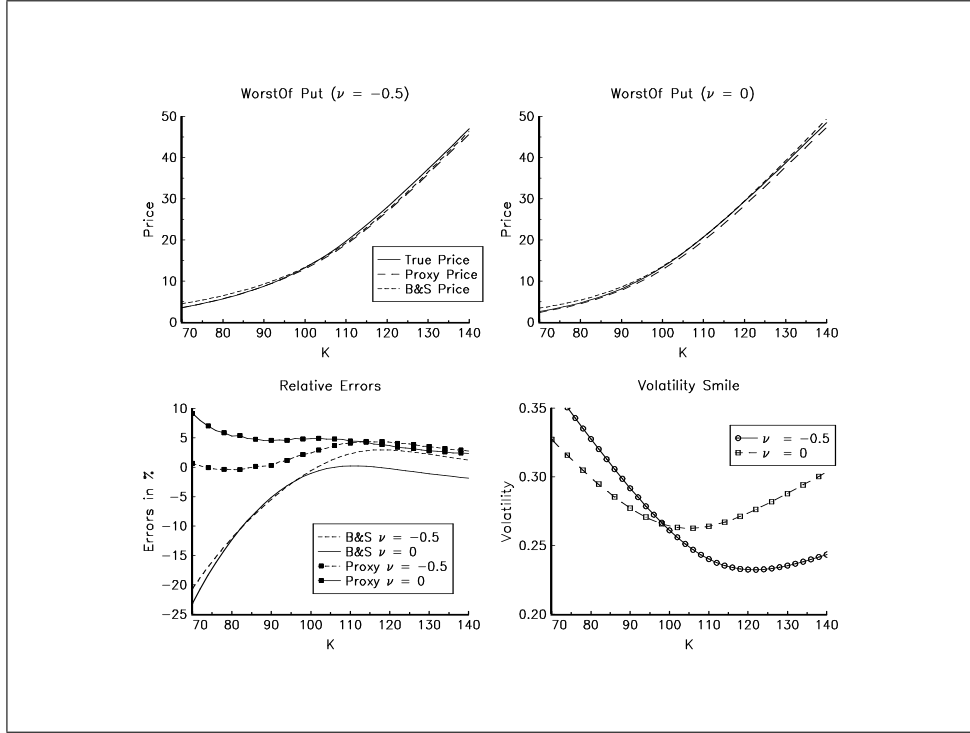


Figure 20: Test of the Proxy for the WorstOf Put/Put option

## 4.2 Greeks computing

One pay generally little attention of the computational aspect of the greek coefficients. However, it is one of the big issue to manage a contingent claims portfolio (EL KAROUI, JEANBLANC and SHREVE [1998]). Let  $C(t_0)$  be a call option price. In the Black and Scholes model, we are interested for example in the delta, gamma and vega coefficients defined by the following derivatives

$$\Delta = \frac{\partial C(t_0)}{\partial S(t_0)}$$

<sup>34</sup>For those simulations, the smile have been generated with the Heston model with

$$\begin{aligned} \kappa &= 0.5 \\ V(\infty) &= 0.3^2 \\ \sigma_V &= 0.9 \\ v &\in \{-0.5; 0\} \end{aligned}$$

Furthermore the maturity of those options have been fixed to one year, the riskless interest rate to 5% and the correlation between the two asset returns to 50%.

$$\begin{aligned}\Gamma &= \frac{\partial^2 C(t_0)}{\partial S^2(t_0)} \\ v &= \frac{\partial C(t_0)}{\partial \sigma}\end{aligned}\tag{86}$$

with  $S(t_0)$  the current price of the underlying asset and  $\sigma$  the volatility. Let  $c(t_0, S(t_0), \sigma)$  be the function corresponding to the price  $C(t_0)$ . If we use a central difference for the first order derivatives, the sensitivities are computed by finite difference as follows<sup>35</sup>

$$\begin{aligned}\Delta_d &= \frac{c(t_0, (1 + \varepsilon) S(t_0), \sigma) - c(t_0, (1 - \varepsilon) S(t_0), \sigma)}{2\varepsilon S(t_0)} \\ \Gamma_d &= \frac{c(t_0, (1 + \varepsilon) S(t_0), \sigma) - 2c(t_0, S(t_0), \sigma) + c(t_0, (1 - \varepsilon) S(t_0), \sigma)}{\varepsilon^2 S^2(t_0)} \\ v_d &= \frac{c(t_0, S(t_0), (1 + \epsilon) \sigma) - c(t_0, S(t_0), (1 - \epsilon) \sigma)}{2\epsilon \sigma}\end{aligned}\tag{88}$$

The theta coefficient is then computed using the PDE formulation

$$\theta = rC(t_0) - bS(t_0) \Delta - \frac{1}{2} \sigma^2 S^2(t_0) \Gamma\tag{89}$$

The use of the previous formula takes some problems when the numerical solution is obtained by MC methods. The first one concerns the *optimal* values of  $\varepsilon$  and  $\epsilon$ . We consider an experiment with an European and a Binary Call options. We use the values of the parameters of the footnote 18 page 11, and different values for  $\varepsilon$ . In some software,  $\varepsilon$  is set to 0.0001. With this value, the delta is well approximated for the vanilla option, but we obtain bad results for the binary option. We remark that there is not a value that will give good results for every option type and all derivatives. In our case,  $\varepsilon = 0.01$  is a suitable choice for the European option, whereas  $\varepsilon = 0.05$  is a better choice for the Binary option.

The second problem concerns the computational time of the finite difference approximation. For example, the gamma needs three Monte Carlo replications. FOURNIÉ, LASRY, LEBUCHOUX, LIONS and TOUZI [1999] present a method to compute the greeks which does not require to run different Monte Carlo replications. This method is based on the Malliavin calculus (NUALART [1995], ØKSENDAL [1996]). Let  $P(t_0) = \mathbb{E}_{\mathbb{Q}} \left[ G(T, X(T)) \exp \left( - \int_{t_0}^T r(t, X(t)) dt \right) \middle| \mathcal{F}_{t_0} \right]$  be the price of an option with the payoff functional  $G$ . FOURNIÉ, LASRY, LEBUCHOUX, LIONS and TOUZI [1999] show that the differentials of  $P(t_0)$  can be expressed as

$$\mathbb{E}_{\mathbb{Q}} \left[ \varpi_{\alpha} G(T, X(T)) \exp \left( - \int_{t_0}^T r(t, X(t)) dt \right) \middle| \mathcal{F}_{t_0} \right]\tag{90}$$

with  $\varpi_{\alpha}$  a random variable and  $\alpha$  the parameter of interest. For example, they obtain the following formulas for the Black-Scholes model<sup>36</sup>

$$\begin{aligned}\Delta_m &= e^{-r(T-t_0)} \mathbb{E}_{\mathbb{Q}} \left[ G(T, S(T)) \frac{W(T)}{\sigma T S(t_0)} \middle| \mathcal{F}_{t_0} \right] \\ \Gamma_m &= e^{-r(T-t_0)} \mathbb{E}_{\mathbb{Q}} \left[ G(T, S(T)) \frac{W^2(T) - \sigma T W(T) - T}{[\sigma T S(t_0)]^2} \middle| \mathcal{F}_{t_0} \right] \\ v_m &= e^{-r(T-t_0)} \mathbb{E}_{\mathbb{Q}} \left[ G(T, S(T)) \frac{W^2(T) - \sigma T W(T) - T}{\sigma T} \middle| \mathcal{F}_{t_0} \right]\end{aligned}\tag{91}$$

<sup>35</sup>In the case of the single-sided forward difference, we have

$$\begin{aligned}\Delta &= \frac{c(t_0, (1 + \varepsilon) S(t_0), \sigma) - c(t_0, S(t_0), \sigma)}{\varepsilon S(t_0)} \\ v &= \frac{c(t_0, S(t_0), (1 + \epsilon) \sigma) - c(t_0, S(t_0), \sigma)}{\epsilon \sigma}\end{aligned}\tag{87}$$

<sup>36</sup>We note that the gamma and the vega are proportional with  $v_m = \sigma T S^2(t_0) \Gamma_m$ .

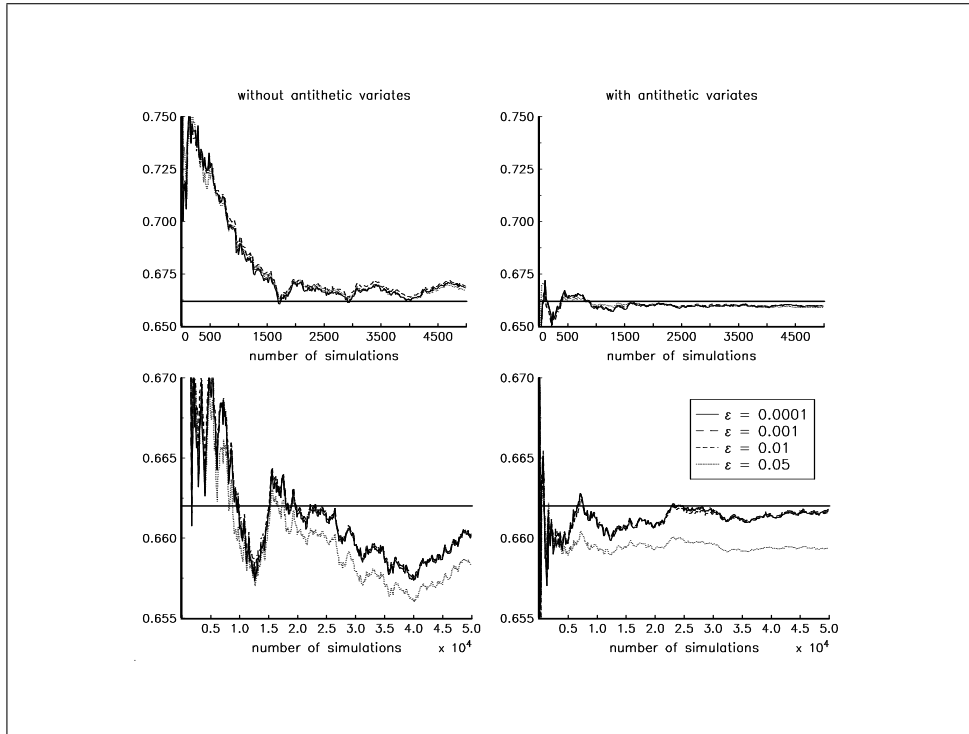


Figure 21:  $\Delta$  for an European Call option

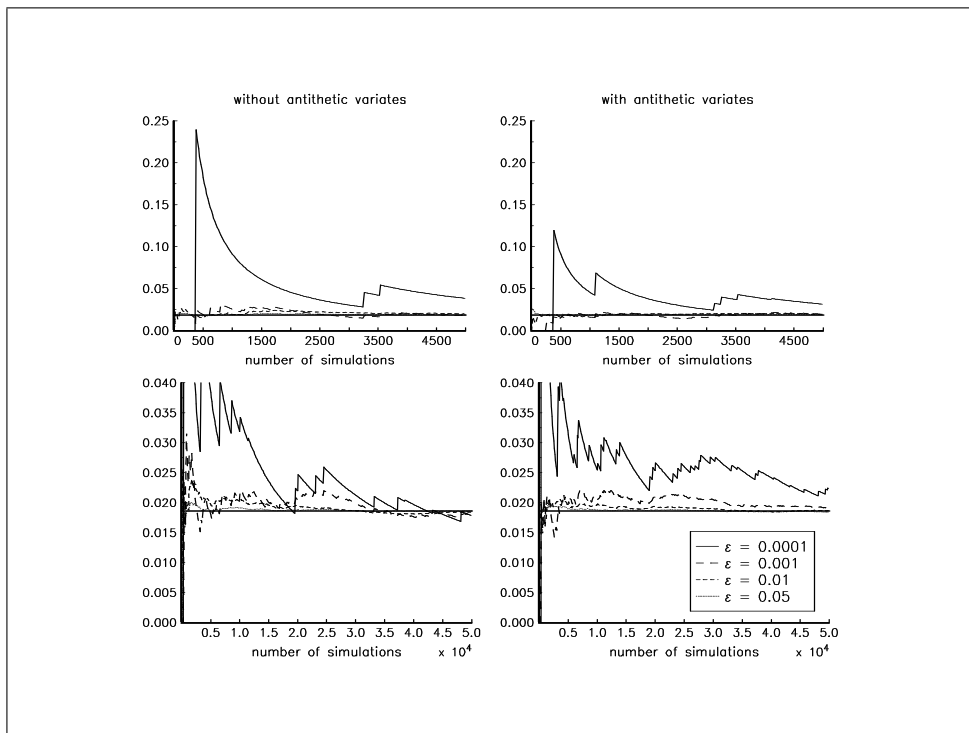


Figure 22:  $\Gamma$  for an European Call option

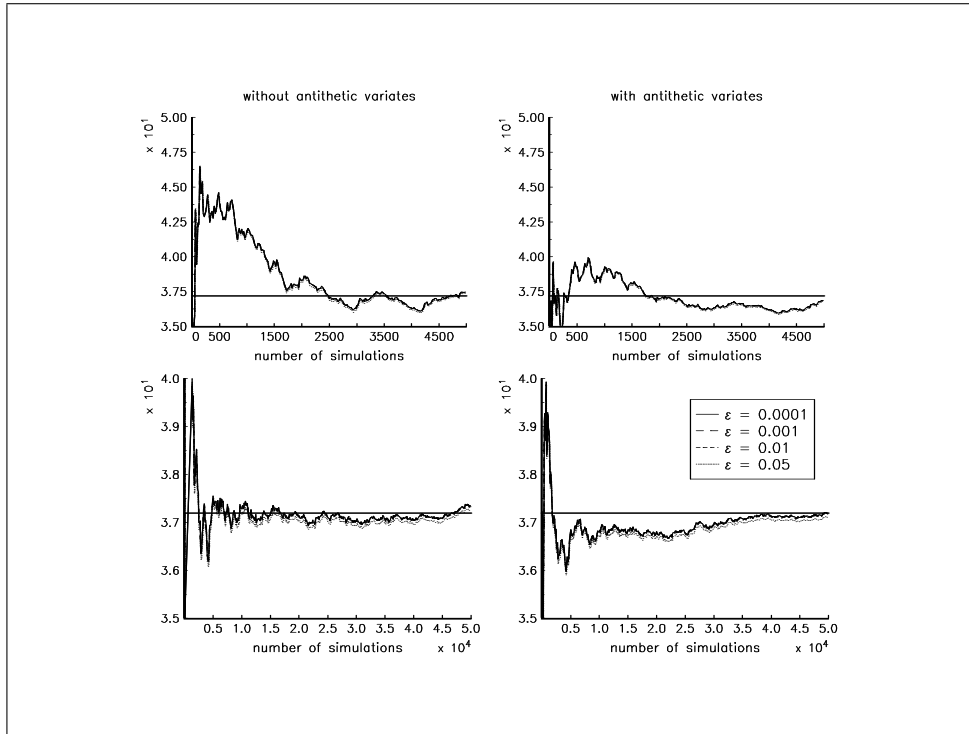


Figure 23:  $v$  for an European Call option

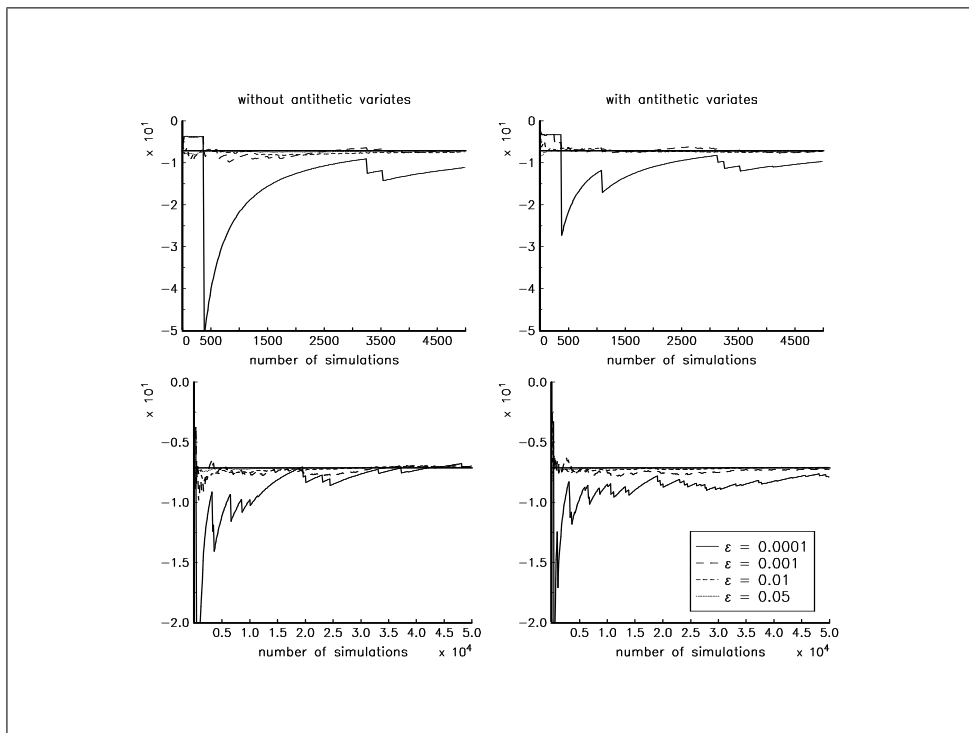


Figure 24:  $\theta$  for an European Call option

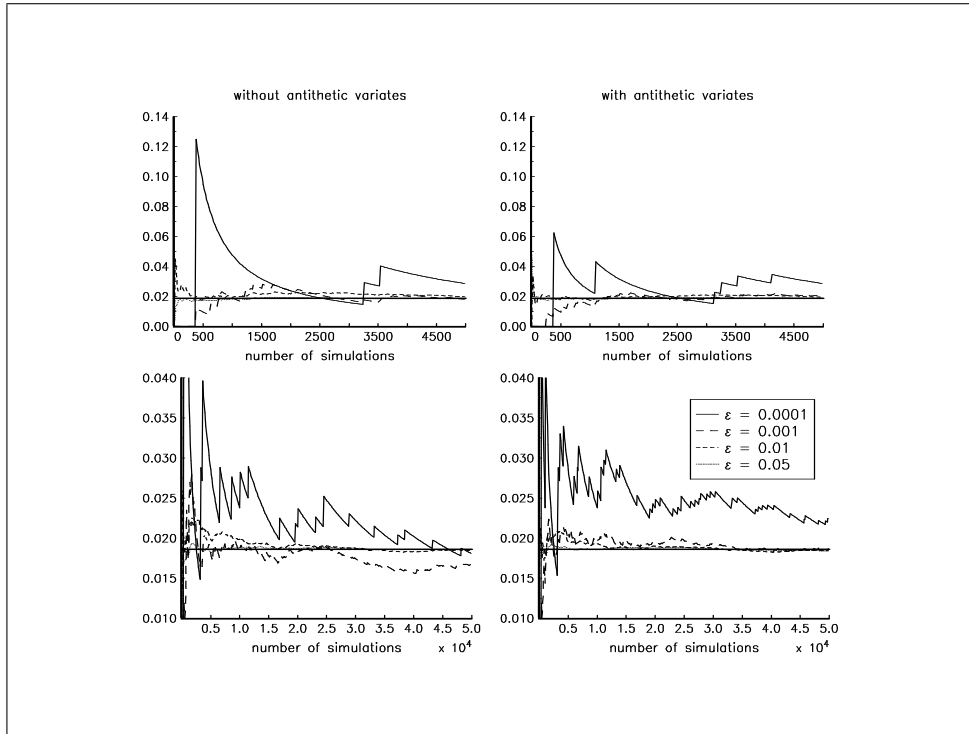


Figure 25:  $\Delta$  for a Binary Call option

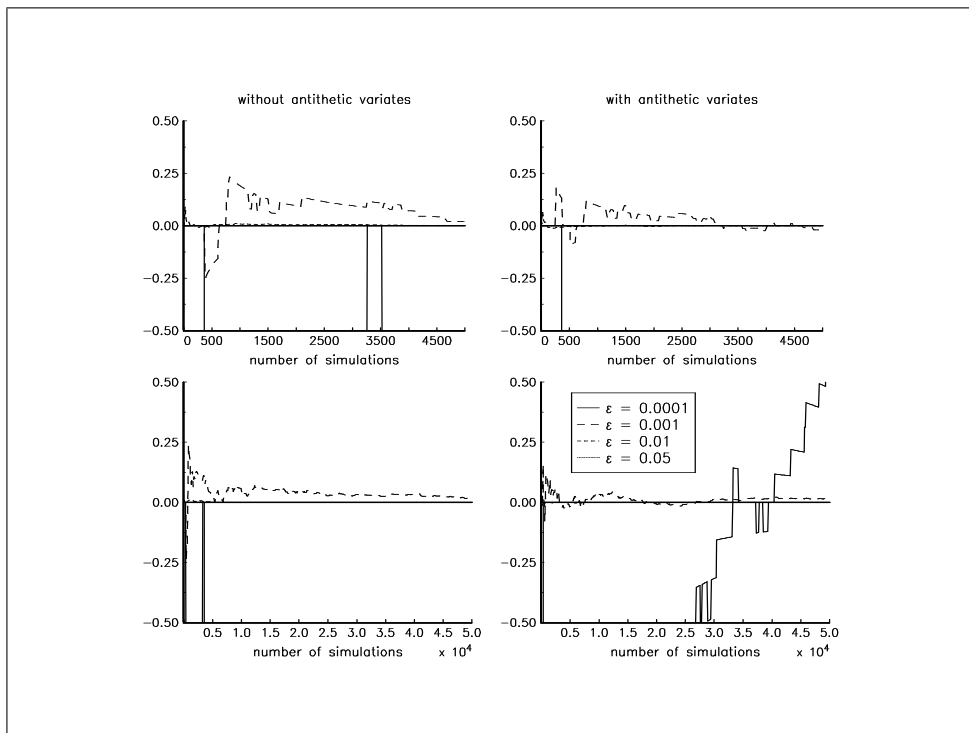


Figure 26:  $\Gamma$  for a Binary Call option

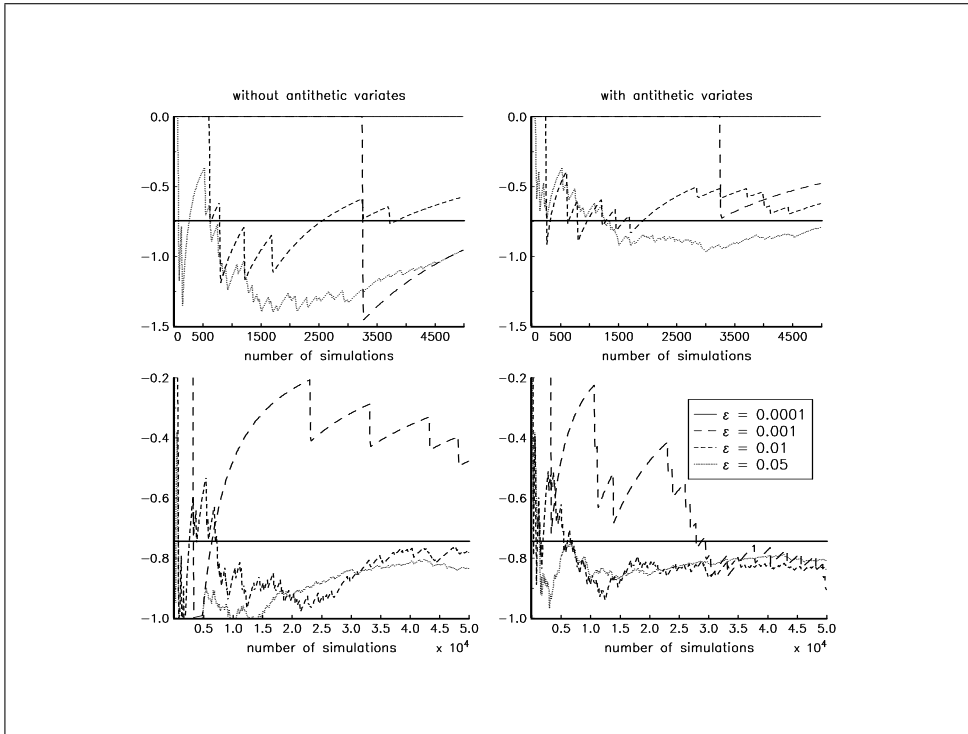


Figure 27:  $v$  for a Binary Call option

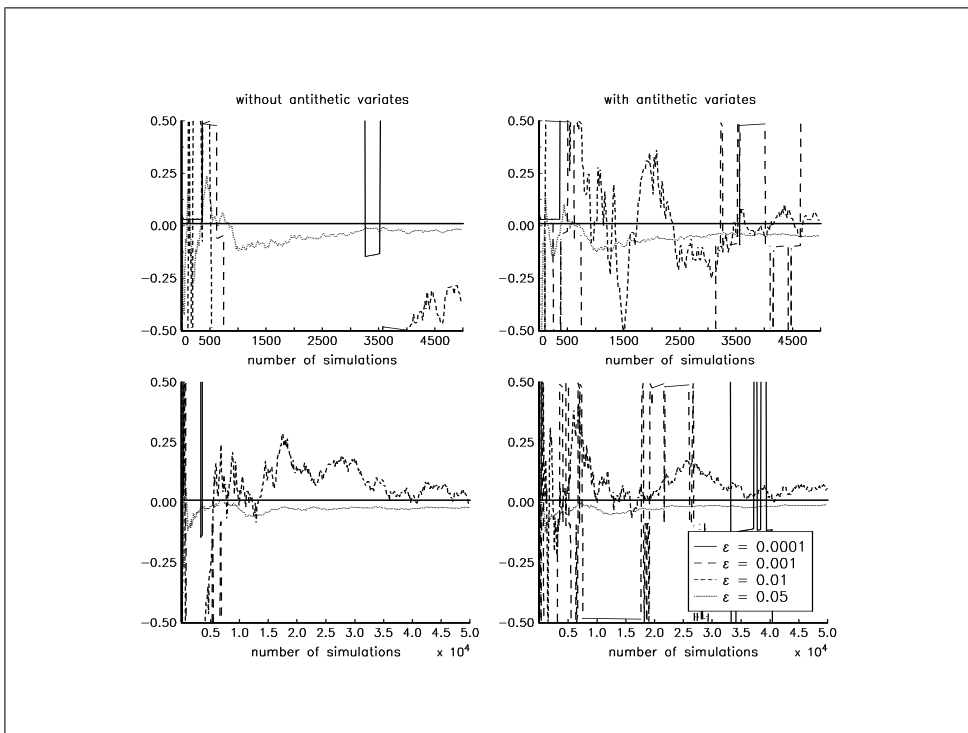


Figure 28:  $\theta$  for a Binary Call option

FOURNIÉ, LASRY, LEBUCHOUX, LIONS and TOUZI [1999] and BENHAMOU [1999b,1999c] remark that “the Malliavin method turns out to be very efficient in the case of discontinuous payoff functionals compared to the Monte Carlo finite difference approach”. The figures (29) and (30) confirm this fact. However, we argue that the most interesting advantage of the Malliavin approach is not the efficiency<sup>37</sup>, but the computational time reduction.

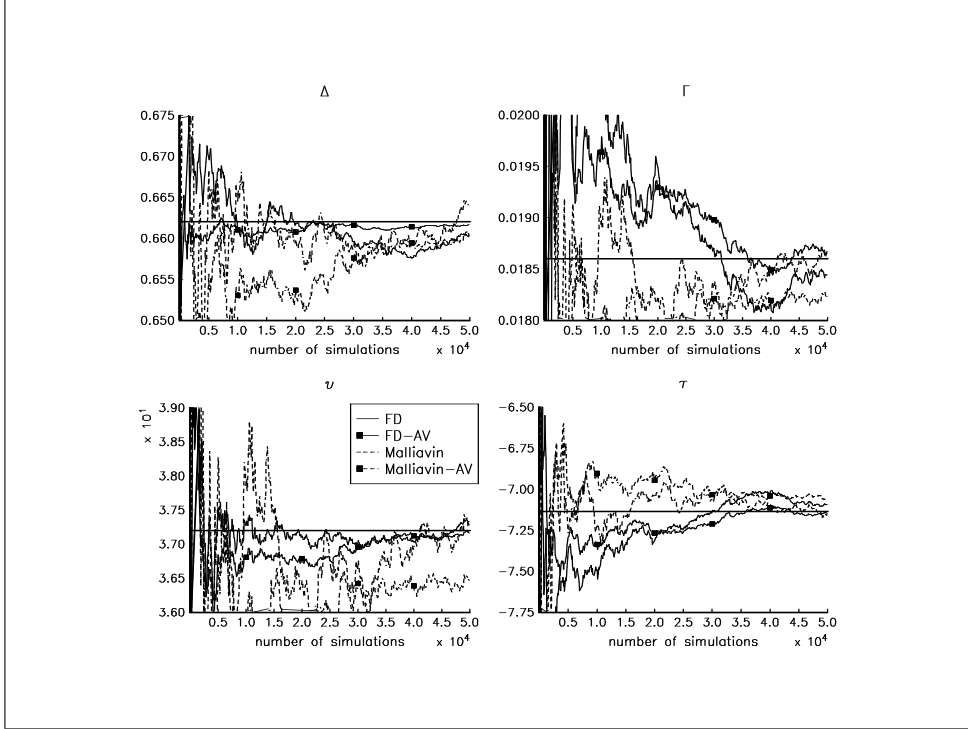


Figure 29: FD vs Malliavin approach — the European Call option example

We could extend the previous results to the case of options with two assets. For example, we have for the delta derivatives

$$\begin{aligned} \Delta_m^1 &= e^{-r(T-t_0)} \mathbb{E}_{\mathbb{Q}} \left[ G(T, S_1(T), S_2(T)) \frac{W_1(T) - \rho W_2(T)}{(1-\rho^2) \sigma_1 T S_1(t_0)} \middle| \mathcal{F}_{t_0} \right] \\ \Delta_m^2 &= e^{-r(T-t_0)} \mathbb{E}_{\mathbb{Q}} \left[ G(T, S_1(T), S_2(T)) \frac{W_2(T) - \rho W_1(T)}{(1-\rho^2) \sigma_2 T S_2(t_0)} \middle| \mathcal{F}_{t_0} \right] \end{aligned} \quad (92)$$

We consider the previous example of the footnote 7 page 5. We consider a Basket option with  $\alpha_1 = 1$ ,  $\alpha_2 = 1$  and  $K = 200$ . We have represented the delta, gamma and vega derivatives for different values of the correlation  $\rho$  — see the figures 31–34. The QMC method uses the Sobol sequence. With this example, we remark that the QMC method gives better results than the MC method. Moreover, the convergence appears very slow for the gamma and vega greeks when  $\rho$  is high in absolute value.

## 5 Conclusion

This paper present different problems on 2D option pricing. Most of the problems concern the numerical algorithm. We have given some illustrations. The main idea is that there is not a unique solution, and that it is not evident that there exist a better solution than others. For each product, we have to do a deep

<sup>37</sup>We have made different simulations, and it is not evident that the Malliavin approach is superior to the finite difference approach.

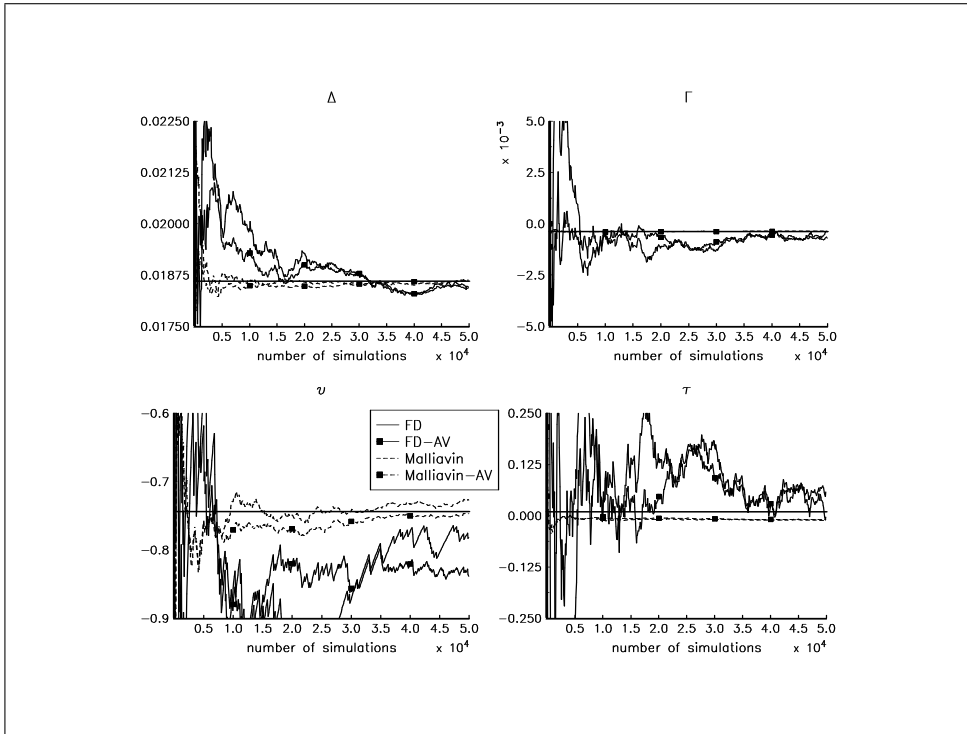


Figure 30: FD vs Malliavin approach — the Binary Call option example

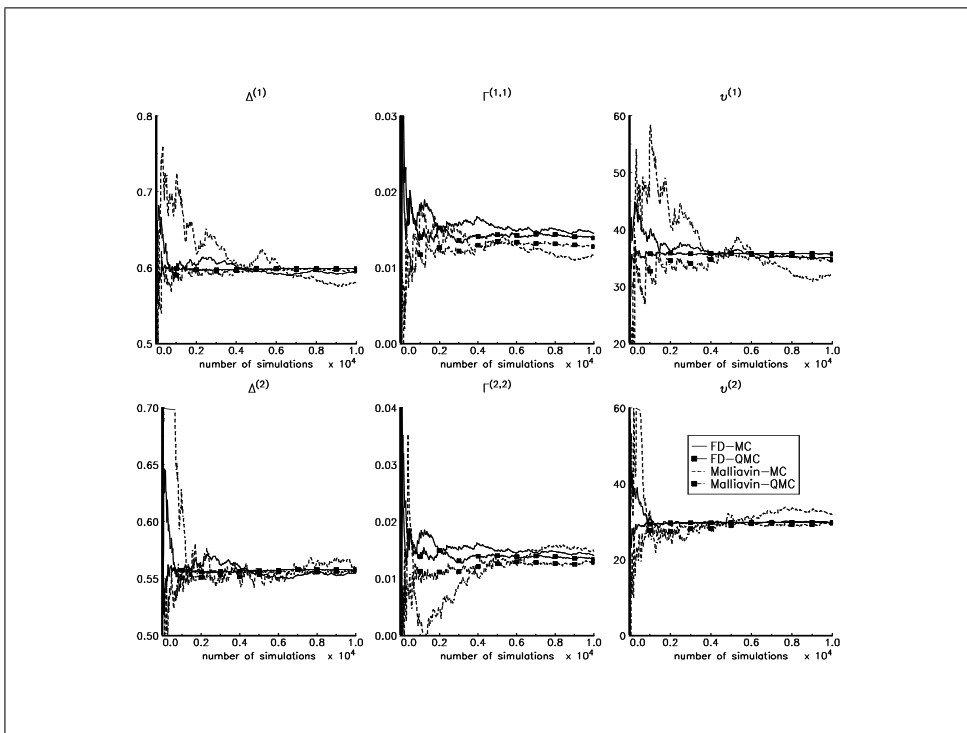


Figure 31: FD vs Malliavin approach —  $\rho = 0.5$

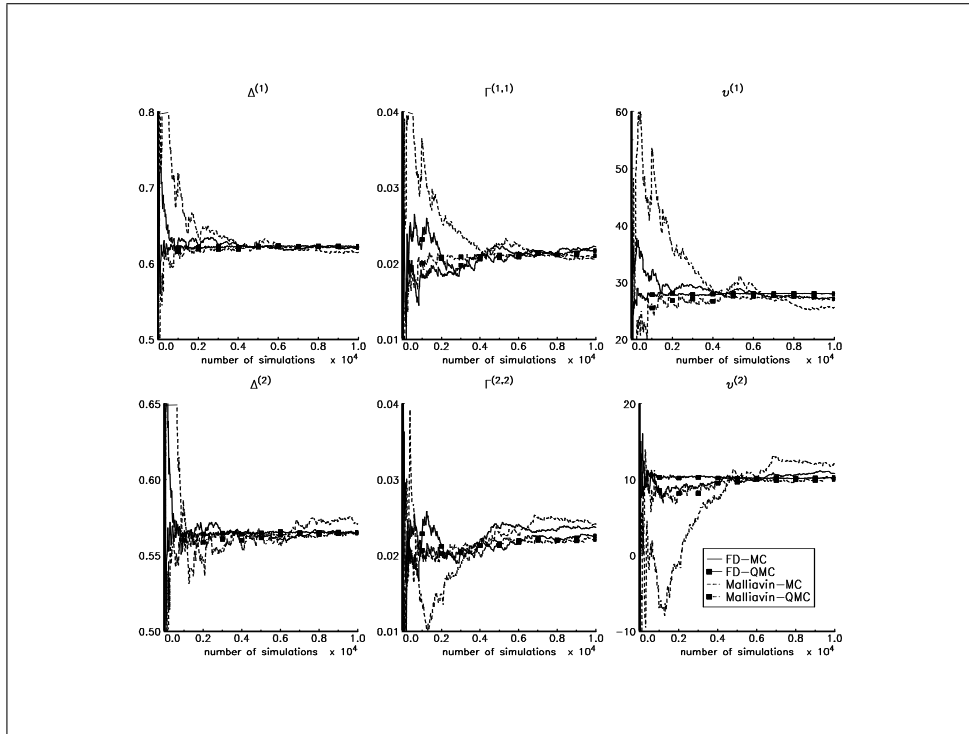


Figure 32: FD vs Malliavin approach —  $\rho = -0.5$

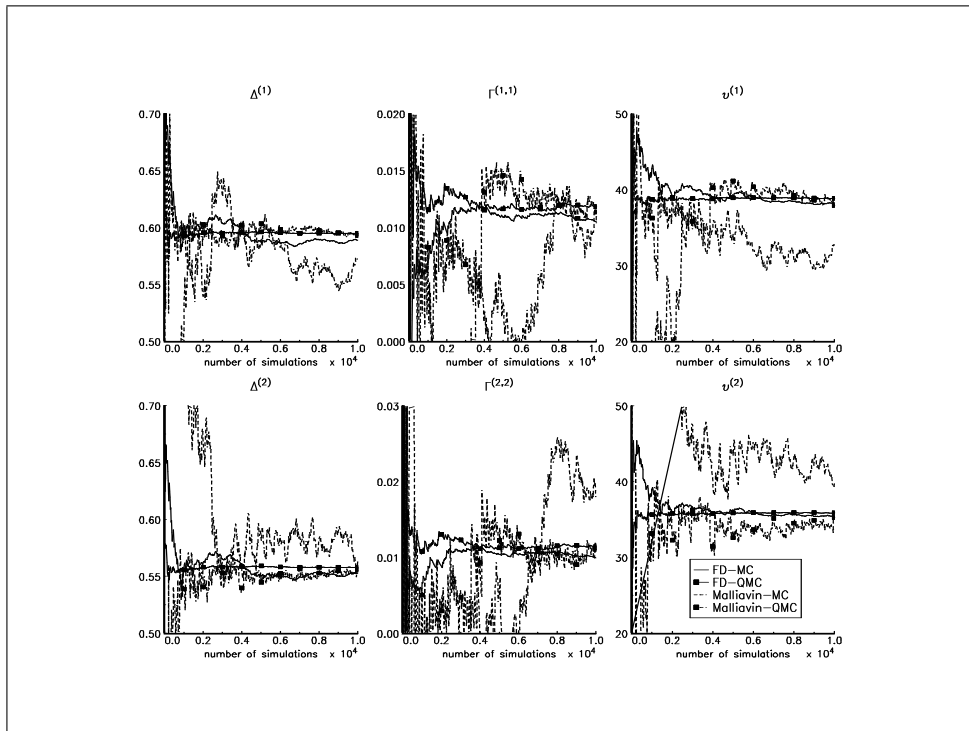


Figure 33: FD vs Malliavin approach —  $\rho = 0.95$

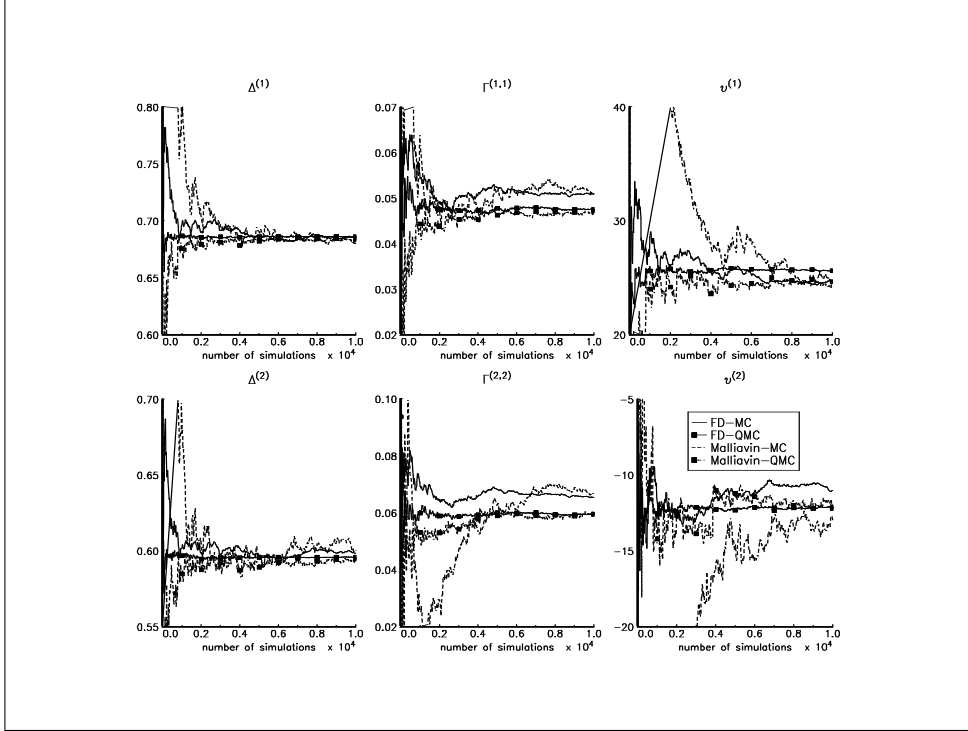


Figure 34: FD vs Malliavin approach —  $\rho = -0.95$

investigation before to choose the appropriate method. And of course, the previous problems become even more complicated in multi-dimensional option pricing.

## Appendix

### A Proof of the Malliavin delta for the two-asset options

We remain that we have

$$\begin{bmatrix} dS_1(t) \\ dS_2(t) \end{bmatrix} = \begin{bmatrix} b_1 S_1(t) \\ b_2 S_2(t) \end{bmatrix} dt + \begin{bmatrix} \sigma_1 S_1(t) & 0 \\ 0 & \sigma_2 S_2(t) \end{bmatrix} \begin{bmatrix} dW_1(t) \\ dW_2(t) \end{bmatrix} \quad (93)$$

with  $E[W_1(t)W_2(t)] = \rho t$ . Let  $S(t) = [S_1(t) \ S_2(t)]^\top$  be the two dimensional process. Let  $Y(t)$  be the related first variation process. The weighting function generator  $\varpi$  is given by the following expression (BENHAMOU [1999a]) :

$$\varpi = \delta(Y(t) \Sigma^{-1}(t, S(t)) \lambda(t)) \quad (94)$$

with  $\delta$  the Skorohod integral and

$$\int_{t_0}^T \lambda(t) \mathcal{X}(t \leq T) dt = 1 \quad (95)$$

One of the difficulty is that this result hold for  $\rho = 0$ . We also introduce the *canonical* Wiener Process  $W^\perp(t) = [W_1^\perp(t) \ W_2^\perp(t)]^\top$  with

$$\begin{cases} W_1^\perp(t) &= W_1(t) \\ W_2^\perp(t) &= (1 - \rho^2)^{-\frac{1}{2}} (W_2(t) - \rho W_1(t)) \end{cases} \quad (96)$$

Then we have<sup>38</sup>

$$\begin{aligned} \varpi &= \frac{1}{T} \begin{bmatrix} (\sigma_1 S_1(t_0))^{-1} & -\rho \left( \sqrt{1-\rho^2} \sigma_1 S_1(t_0) \right)^{-1} \\ 0 & \left( \sqrt{1-\rho^2} \sigma_2 S_2(t_0) \right)^{-1} \end{bmatrix} W^\perp(T) \\ &= \begin{bmatrix} \left( \sqrt{1-\rho^2} W_1^\perp(T) - \rho W_2^\perp(T) \right) \left( \sqrt{1-\rho^2} \sigma_1 T S_1(t_0) \right)^{-1} \\ W_2^\perp(T) \left( \sqrt{1-\rho^2} \sigma_2 S_2(t_0) \right)^{-1} \end{bmatrix} \end{aligned} \quad (97)$$

Using the relationship (96), we obtain the desired formula (92).

## References

- [1] ABRAMOWITZ, M. and I.A. STEGUN [1970], Handbook of Mathematical Functions, ninth edition, Dover
- [2] BAKSHI, G., C. CAO and Z. CHEN [1997], Empirical performance of alternative option pricing models, *Journal of Finance*, **52**, 2003-2049
- [3] BARLES, G., J. BURDEAU, M. ROMANO and N. SAMSOEN [1992], Critical stock price near expiration, *Mathematical Finance*, **5**, 77-96
- [4] BARRETT, R., M. BERRY, T. F. CHAN, J. DEMMEL, J. DONATO, J. DONGARRA, V. EIJKHOUT, R. POZO, C. ROMINE and H. VORST (Van der) [1994], Templates for the Solution of Linear Systems: Building Blocks for Iterative Methods, 2nd Edition, SIAM, Philadelphia, PA
- [5] BENHAMOU, E. [1999a], Reducing the variance in Monte Carlo and quasi-Monte Carlo simulations for the greeks using Malliavin calculus, London School of Economics, *Working Paper*
- [6] BENHAMOU, E. [1999b], Explicit faster greeks for strong non-linear payoff options in Black world, London School of Economics, *Working Paper*
- [7] BENHAMOU, E. [1999c], An application of Malliavin calculus to Asian and Lookback options' greeks, London School of Economics, *Working Paper*
- [8] BENSOUSSAN, A. [1984], On the theory of option pricing, *Acta Applicandae Mathematicae*, **2**, 139-158
- [9] BERMIN, H-P. and A. KOHATSU-HIGA [1999], Local volatility changes in the Black-Scholes model, Department of Economics, Lund University, *Working Paper*
- [10] BIRGE, J.R. [1994], Quasi-Monte Carlo approaches to option pricing, Department of Industrial and Operations Engineering, University of Michigan, *Technical Report*, **94-19**
- [11] BOULEAU, N. and D. LÉPINGLE [1994], Numerical methods for stochastic processes, *Wiley Series in Probability and Mathematical Statistics*, John Wiley & Sons, New York
- [12] BRATLEY, P. and B.L. FOX [1988], ALGORITHM 659 implementing Sobol's quasirandom sequence generator, *ACM Transactions on Mathematical Software*, **14**, 88-100
- [13] BRATLEY, P., B.L. FOX and H. NIEDERREITER [1988], Implementation and tests of low-discrepancy sequences, *ACM Transactions on Modeling and Computer Simulation*, **2**, 195-213
- [14] BUSCA, J. [1999], A finite element method for the valuation of American options, C.A.R., *Research Report*
- [15] CAFLISCH, R.E., W. MOROKOFF and A.B. OWEN [1997], Valuation of mortgage securities using brownian bridges to reduce effective dimension, Department of Mathematics, UCLA, *Technical report*

---

<sup>38</sup>We use the trivial solution  $\lambda(t) = t^{-1}$ .

- [16] CALVETTI, D., G.H. GOLUB, W.B. GRAGG and L. REICHEL [1998], Computation of Gauss-Kronrod quadrature rules, Stanford University Scientific Computing, *Computational Mathematics Report*, **SCCM-98-09**
- [17] CHERNOV, M. and E. GHYSELS [1999], A study towards a unified approach to the joint estimation of objectiven and risk neutral measures for the purpose of options valuations, Pennsylvania State University, *Working Paper*
- [18] DAVIS, P.J. and P. RABINOWITZ [1984], *Methods of Numerical Integration*, second edition, Academic Press, Orlando
- [19] DETEMPLE, J., R. GARCIA and M. RINDISBACHER [2000], A Monte Carlo method for optimal portfolios, CIRANO, *Working Paper*, **2000s-05**
- [20] EL KAROUI, N., M. JEANBLANC and S.E. SHREVE [1998], On the robustness of the Black-Scholes equation, *Mathematical Finance*, **8**, 93-126
- [21] ENTACHER, K. [1998], A collection of selected pseudorandom number generators with linear structures, Department of Mathematics, University of Salzburg, *Working Paper*
- [22] FORNBERG, B. [1998], Calculation of weights in finite difference formulas, *SIAM Review*, **40**, 685-691
- [23] FOURNIÉ, E., J-M. LASRY, J. LEBUCHOUX, P-L. LIONS and N. TOUZI [1999], Applications of Malliavin calculus to Monte Carlo methods in finance, *Finance & Stochastics*, **3**, 391-412
- [24] FOURNIÉ, E., J-M. LASRY, J. LEBUCHOUX and P-L. LIONS [1999], Applications of Malliavin calculus to Monte Carlo methods in finance II, CEREMADE, *Working Paper*, **9901**
- [25] FOX, G.C., MESSINA, P.C. and R.D. WILLIAMS [1994], *Parallel Computing Works!*, Morgan Kaufmann Publishers, San Francisco
- [26] FRIEDMAN, A. [1975], *Stochastic Differential Equations and Applications*, volume I, Academic Press, New York
- [27] GEWEKE, J. [1996], Monte Carlo simulation and numerical integration, in H. Amman, D. Kendrick and J. Rust (eds.), *Handbook of Computational Economics*, North-Holland, Amsterdam, 731-800
- [28] GOLUB, G.H. and J. ORTEGA [1993], *Scientific Computing: An Introduction with Parallel Computing*, Academic Press
- [29] GOLUB, G.H. and C.F. VAN LOAN [1989], *Matrix Computations*, second edition, Johns Hopkins University Press
- [30] GOLUB, G.H. and J.H. WELSCH [1969], Calculation of the Gauss quadrature rules, *Mathematics of Computation*, **23**, 221-230
- [31] GOURLAY, A.R. [1970], Hopscotch: a fast second-order partial differential equation solver, *Journal of the Institute of Mathematics and Applications*, **6**, 375-390
- [32] GOURLAY, A.R. and S. MCGUIRE [1971], General hopscotch algorithm for the numerical solution of partial differential equations, *Journal of the Institute of Mathematics and Applications*, **7**, 216-227
- [33] GOURLAY, A.R. and S. MCKEE [1977], The construction of hopscotch methods for parabolic and elliptic equations in two space dimensions with a mixed derivative, *Journal of Computational and Applied Mathematics*, **3**, 201-205
- [34] HARRISON, J.M. and S.R. PLISKA [1981], Martingales and stochastic integrals in the theory of continuous trading, *Stochastic Processes and their Applications*, **11**, 215-260
- [35] HARRISON, J.M. and S.R. PLISKA [1983], A stochastic calculus model of continuous trading: complete markets, *Stochastic Processes and their Applications*, **15**, 313-316

- [36] HESTON, S.L. [1993], A closed-form solution for options with stochastic volatility with application to bond and currency options, *Review of Financial Studies*, **6**, 327-343
- [37] HULL, J.C. and A. WHITE [1987], The pricing of options on assets with stochastic volatilities, *Journal of Finance*, **42**, 281-300
- [38] IPSEN, I.C.F. and C.D. MEYER [1998], The idea behind Krylov methods, *American Mathematical Monthly*, **105**, 889-899
- [39] KARATZAS, I. [1988], On the pricing of American options, *Applied Mathematics and Optimisation*, **17**, 37-60
- [40] KIM, I. [1990], The analytic valuation of American options, *Review of Financial Studies*, **3**, 547-572
- [41] KURPIEL, A. and T. RONCALLI [1999], Hopscotch methods for two-state financial models, *Journal of Computational Finance*, **3**, 53-89
- [42] KURPIEL, A. [1999], American options exercise policy in a stochastic volatility model, Université Montesquieu-Bordeaux IV, GRAPE, *Working Paper*
- [43] KURPIEL, A. [2000], Estimation des paramètres des modèles à volatilité stochastique, Université Montesquieu-Bordeaux IV, GRAPE, *Working Paper*
- [44] LEMIEUX, C. and P. L'ECUYER [2000], A comparison of Monte Carlo, lattice rules and other low-discrepancy point sets, in H. Niederreiter and J. Spanier (eds.), *Monte Carlo and Quasi-Monte Carlo Methods 1998*, Springer, Berlin
- [45] LEVEQUE, R.J. [1998], Finite Difference Methods for Differential Equations, Department of Applied Mathematics, University of Washington, *Lecture Notes*
- [46] MAKIVIC, M. [1995], Path integral Monte Carlo method for valuation of derivative securities: Algorithm and parallel implementation, *Neural Network World*, **5**, 503-524
- [47] MEYER, G.H. and J. HOEK (van der) [1997], The valuation of american options with the method of lines, *Advances in Futures and Options Research*, **9**, 265-285
- [48] MOERBEKE (van), P.L.J. [1976], On optimal stopping and free boundary problems, *Archive for Rational Mechanics and Analysis*, **60**, 101-148
- [49] MOROKOFF, W. and R.E. CAFLISCH [1994], Quasi-random sequences and their discrepancies, *SIAM Journal on Scientific and Statistical Computing*, **15**, 1251-1279
- [50] MOROKOFF, W. and R.E. CAFLISCH [1995], Quasi-Monte Carlo integration, *Journal of Computational Physics*, **122**, 218-230
- [51] NUALART, D. [1995], Malliavin Calculus and Related Topics, *Probability and its Applications*, Springer, Berlin
- [52] ØKSENDAL, B. [1996], An introduction to Malliavin calculus with applications to economics, Norwegian School of Economics and Business Administration, *Working Paper*, **3/96**
- [53] ÖKTEN, G. [2000], Applications of a Hybrid-Monte Carlo sequence to option pricing, in H. Niederreiter and J. Spanier (eds.), *Monte Carlo and Quasi-Monte Carlo Methods 1998*, Springer, Berlin
- [54] OWEN, A.B. [1998a], Scrambling Sobol and Niederreiter-Xing points, *Journal of Complexity*, **14**, ??
- [55] OWEN, A.B. [1998b], Latin supercube sampling for very high dimensional simulations, *ACM Transactions on Modeling and Computer Simulation*, **8**, 71-102
- [56] PAIGE, C.C. and M.A. SAUNDERS [1982a], LSQR: An algorithm for sparse linear equations and sparse least squares, *ACM Transactions on Mathematical Software*, **8**, 43-71

- [57] PAIGE, C.C. and M.A. SAUNDERS [1982b], Algorithm 583; LSQR: Sparse linear equations and least-squares problems, *ACM Transactions on Mathematical Software*, **8**, 195-209
- [58] PAPAGEORGIOU, A. and J.F. TRAUB [1996], Beating Monte Carlo, *Risk*, June, 63-65
- [59] PAPAGEORGIOU, A. and J.F. TRAUB [1997], Faster evaluation of multidimensional integrals, *Computers in Physics*, **11**, 574-578
- [60] PASKOV, S.H. [1994], Computing high dimensional integrals with applications to finance, Summer Research Conference on Continuous Algorithms and Complexity, Mount College, June
- [61] PASKOV, S.H. and J.F. TRAUB [1995], Faster valuation of financial derivatives, *Journal of Portfolio Management*, **22**, 113-120
- [62] PRESS, W.H., S.A. TEUKOLSKY, W.T. VETTERLING and B.P. FLANNERY [1992], Numerical Recipes in Fortran, second edition, Cambridge University Press, Cambridge
- [63] ROMANO, M. and N. TOUZI [1997], Contingent claims and market completeness in a stochastic volatility model, *Mathematical Finance*, **7**, 399-412
- [64] RONCALLI, T. and A. KURPIEL [1998], A GAUSS implementation of Hopscotch methods — the PDE2D library, FERC, City University Business School
- [65] SAAD, Y. [1996], Iterative Methods for Sparse Linear Systems, PWS Publishing Company, Boston
- [66] SAAD, Y. [1998], Workshop on Numerical Methods for Large Scale Linear Systems of Equations, Australian National University, Canberra, Australia, Nov. 16-20, *Lecture Notes*
- [67] SCHUSS, Z. [1980], Theory and Applications of Stochastic Differential Equations, John Wiley & Sons, New York
- [68] SCOTT, L. [1987], Option pricing when the variance changes randomly: theory, estimation and an application, *Journal of Financial and Quantitative Analysis*, **22**, 419-438
- [69] SLOAN, I.H. and H. WOŹNIAKOWSKI [1998], When are Quasi-Monte Carlo algorithms efficient for high-dimensional integrals?, *Journal of Complexity*, **14**, 1-33
- [70] SPANIER, J. and L. LI [1998], Quasi-Monte Carlo methods for integral equations, in H. Niederreiter, P. Hellekalek, G. Larcher and P. Zinterhof (eds.), *Monte Carlo and Quasi-Monte Carlo Methods 1996, Lectures Notes in Statistics*, **127**, Springer, New York
- [71] STOER, J. and R. BULIRSCH [1993], Introduction to Numerical Analysis, second edition, *Texts in Applied Mathematics*, **12**, Springer, New York
- [72] THIÉMARD, E. [1998], Economic generation of low-discrepancy sequences with a  $b$ -ary Gray Code, Ecole Polytechnique Fédérale de Lausanne, Département de Mathématiques, *Working Paper*
- [73] TRAUB, J.F. and H. WOŹNIAKOWSKI [1992], The Monte Carlo algorithm with a pseudo-random generator, *Mathematics of Computation*, **58**, 303-339
- [74] TOUZI, N. [1999], American options exercise boundary when the volatility changes randomly, *Applied Mathematics and Optimisation*, **39**, 411-422
- [75] VILLENEUVE, S. and A. ZANETTE [1998], Parabolic A.D.I. methods for pricing American options on two stocks, Université de Marne-La-Vallée, *Working Paper*, **25/98**
- [76] WIGGINS, J.B. [1987], Option values under stochastic volatility, *Journal of Financial Economics*, **19**, 351-372
- [77] WILMOTT, P., J. DEWYNNE and S. HOWISON [1993], Option Pricing: Mathematical Models and Computation, Oxford Financial Press, Oxford, England